



Norwegian  
Meteorological  
Institute

METreport

No. X/2016

ISSN 2387-4201

Oceanography

# Evaluation of the FjordOs-model

July 2016

Karina Hjellevik<sup>1</sup>, André Staalstrøm<sup>2</sup>, Nils M. Kristensen<sup>3</sup>, Lars P. Røed<sup>3,4</sup>



<sup>1</sup>University College of Southeast Norway, <sup>2</sup>Norwegian Institute for Water Research,

<sup>3</sup>Norwegian Meteorological Institute, <sup>4</sup>Department of Geosciences, University of Oslo



Norwegian  
Meteorological  
Institute

# METreport

<b>Title</b>	<b>Date</b>
Evaluation of the FjordOs-model	February 7, 2017
<b>Section</b>	<b>Report no.</b>
Ocean and Ice	X/2015
<b>Author(s)</b>	<b>Classification</b>
Karina Hjelmervik, Nils Melsom Kristensen, André Staalstrøm, Lars Petter Røed	<input checked="" type="radio"/> Free <input type="radio"/> Restricted
<b>Client(s)</b>	<b>Client's reference</b>
Oslofjordfondet	
<b>Abstract</b>	Provided is an evaluation on the performance of the FjordOs model, a new circulation model covering the Oslofjord, Norway. The model is developed to improve the ocean input (e.g., currents) to emergency models used to predict pathways of oil and/or other effluents. The FjordOs model is a regional adaption of the Regional Ocean Modeling System (ROMS), and makes use of the model's curvilinear option to increase the resolution without inflating the computer demand significantly. The observations encompass water level, currents and temperature at various time periods and fixed stations, and observed trajectories of drifters. To assess the model's rendition of the circulation we compare results from a simulation for the two years 2014 and 2015 to available observations. The evaluation reveals that the model is not perfect, but nevertheless we contend that its performance is adequate for its purpose. An important justification is that the higher resolution offers a decrease in the number of stranded trajectories compared to models of coarser resolution. Also of importance is that the model provides a realistic depth profile of the currents, and the tidal elevation.
<b>Keywords</b>	Ocean model, Oslofjord, ROMS, Validation, Fjordos

## Abstract

Provided is an evaluation on the performance of the FjordOs model, a new circulation model covering the Oslofjord, Norway. The model is developed to improve the ocean input (e.g., currents) to emergency models used to predict pathways of oil and/or other effluents. The FjordOs model is a regional adaption of the Regional Ocean Modeling System (ROMS), and makes use of the model's curvilinear option to increase the resolution without inflating the computer demand significantly. The observations encompass water level, currents and temperature at various time periods and fixed stations, and observed trajectories of drifters. To assess the model's rendition of the circulation we compare results from a simulation for the two years 2014 and 2015 to available observations. The evaluation reveals that the model is not perfect, but nevertheless we contend that its performance is adequate for its purpose. An important justification is that the higher resolution offers a decrease in the number of stranded trajectories compared to models of coarser resolution. Also of importance is that the model provides a realistic depth profile of the currents, and the tidal elevation.

# Contents

<b>1</b>	<b>Introduction</b>	<b>1</b>
<b>2</b>	<b>The Oslofjord and the FjordOs model</b>	<b>2</b>
<b>3</b>	<b>Observations</b>	<b>5</b>
3.1	Water level . . . . .	6
3.2	Currents . . . . .	6
3.2.1	Currents in two cross sections . . . . .	6
3.2.2	Currents at Slagentangen . . . . .	8
3.3	Hydrography . . . . .	9
3.3.1	CTD measurements . . . . .	9
3.3.2	Water temperature near Åsgårdstrand . . . . .	9
3.3.3	Water temperature in the Inner Oslofjord . . . . .	11
3.4	Drifters and oil drift . . . . .	12
3.4.1	Godafoss oil spill . . . . .	12
3.4.2	Surface drifters . . . . .	13
<b>4</b>	<b>Evaluation</b>	<b>15</b>
4.1	Water level and tide . . . . .	15
4.2	Currents . . . . .	19
4.2.1	Currents in two cross sections . . . . .	19
4.2.2	Current at Slagentangen . . . . .	22
4.3	Hydrography . . . . .	25
4.3.1	CTD-measurements . . . . .	25
4.3.2	Water temperature near Åsgårdstrand . . . . .	33
4.3.3	Water temperature in the Inner Oslofjord . . . . .	36
4.4	Drifting lanes . . . . .	38
4.4.1	Godafoss . . . . .	38
4.4.2	Surface drifters . . . . .	41
<b>5</b>	<b>Summary and final remarks</b>	<b>48</b>
<b>Acknowledgements</b>		<b>49</b>

**Appendix** **50**

**References** **54**

# 1 Introduction

We assess the performance of a new regional circulation model developed specifically for the Oslofjord, Norway. The model is named FjordOs and is a version of the Regional Ocean Model System (ROMS) adapted for the fjord utilizing its curvilinear option. For details on the FjordOs model, the reader is referred to *Røed et al.* (2016).

The motivation is to construct a model with high enough resolution to properly resolve the fjord's many small islands, narrow straits and sounds, and to resolve its highly irregular coastline and topography 1. The hypothesis is that such a resolution is necessary to avoid effluents to be stranded artificially when simulating their pathways from the source. As is well known currents, besides wind and waves, is one of the dominant sources when predicting pathways of effluents like oil and/or discharges of other contaminants. Thus, the FjordOs model is designed to deliver simulation and/or forecasts of water level, current, temperature and salinity accurate enough to be a useful input to drift models.

The study is a part of the FjordOs project. FjordOs is a cooperation between MET Norway, University College of Southeast Norway (HSN), The Norwegian Institute for Water Research (NIVA), The Norwegian Coastal Administration (Kystverket), Exxonmobil, Norwegian Defence Research Establishment (FFI), Vestfold, Buskerud, and Østfold county, and AGNES AB Miljøkonsulent.

The evaluation is based on available observations for the two year period 2014 and 2015 for which simulations with the FjordOs model is performed. Most of the observations are gathered from different sources independent of the FjordOs project, and include measurements of water level, currents, and water temperature at fixed station in addition to CTD measurements scattered in time and space. In addition a short scientific cruise on board the research vessel (R/V) Trygve Braarud was conducted as part of the FjordOs project in September 2015 to provide additional observations of hydrography and not least trajectories of drifters (*Hjelmervik et al.*, 2016). Finally, some observations were performed close to Svelvik in 2015 in the Drammensfjord, a western branch of the main Oslofjord (*Staalstrøm and Hjelmervik*, 2017).

While Section 2 gives a brief introduction to the Oslofjord and the model, more details on the observations are offered in Section 3. The assessment of the model's performance is presented in Section 4, while a summary including conclusions and some final remarks are proffered in Section 5. Some calculations on driftling lanes from the Slagen refinery are added in the Appendix.

## 2 The Oslofjord and the FjordOs model

The area of interest, and the domain covered by the model FjordOs, is the Oslofjord including the Drammensfjord and the Inner Oslofjord (Fig. 1). The fjord is located in southeastern Norway and is well described in the literature, e.g., *Baalsrud and Magnusson* (2002), *Røed et al.* (2016), and *Hjelmervik et al.* (2017). Here we only point out some salient facts to keep in mind when establishing a circulation model aimed at providing pathways of various effluents to the fjord.

As revealed by Figure 1, the fjord is rather long and narrow with occasional wider parts. At about  $59.5^{\circ}\text{N}$  the fjord splits in two branches. A western branch tapers into a narrow strait at Svelvik before it opens up a bit to form the Drammensfjord. An eastern branch forms the long and narrow Drøbak Sound, before it also opens up to form the somewhat wider Inner Oslofjord with its characteristic "swan head". In the north south direction it is about 100 km long. At the entrance it is about 50 km wide, in the Drøbak Sound about 1-2 km, and as narrow as 180 meters at Svelvik.

Both branches have a sill. The sill in the eastern branch, the Drøbak Sill, is located close to the island Kaholmen which holds the citadel Oscarsborg. It consists partly of a man made underwater jetty only 1-2 meters deep extending halfway across the fjord from the western side. East of the jetty there is a natural sill of about 20 meters depth. Due its narrowness and shallowness the Drøbak Sill area is famous for its strong tidal currents, which easily exceeds 1 m/s even though the mean total tidal amplitude is less than 20 cm. The sill in the western branch is rather long and narrow, about 1 km long and 180 meters wide. The minimum depth is as shallow as 11 meters. This sill also causes a strong tidal current called the Svelvikstraum. North of the sills the maximum depth is more than 120 meters in both branches.

In addition to the existence of many small and large islands giving rise to many narrow sounds and straits, the fjord also have several deep basins ranging from 190 to 400 meters depths. Moreover, the fjord also exhibit a rather irregular coastline, and several rivers discharging fresh water into the fjord. Among the latter are two of Norway's largest rivers, namely Glomma (near Fredrikstad) and Drammenselva (near Drammen). An important contributer to the water level variations and thereby the circulation pattern in the fjord is the impact of events in the Skagerrak/North Sea through the Oslofjord's southern perimeter. For instance are storm surge events with amplitudes of one meter and higher observed in the fjord, which are associated with wind and pressure events in the Skagerrak/North

These complexities all contributes to a compounded circulation pattern, a pattern that is important to resolve when designing a circulation model for the fjord aimed at providing as realistic as possible pathways of effluents. To conceivably account for all these complexities and at the same time not exceeding the available computer capacities we opted to adapt the Rutgers Regional Ocean Modeling System (ROMS) when constructing the model for the Oslofjord, and to exploit its curvilinear option. ROMS is a publicly available ocean model featuring a terrain-following vertical coordinate and a free-surface. It is well documented by *Haidvogel et al.* (2008) and by *Shchepetkin and McWilliams* (2003, 2005, 2009). The particular version adapted to the Oslofjord is called FjordOs. For details on the FjordOs model and the simulations performed for the two years 2014 and 2015 the reader is referred to *Røed et al.* (2016). The latter also describes the setup including the applied external inputs, such as atmospheric input, river input, tidal input, and the input of sea level, currents and hydrography at the model's open lateral southern boundary.

Finally we emphasize that since ROMS is a terrain-following model it is plagued by currents created by the inescapable pressure gradient errors (). To minimize its effect we have, as is common, smoothed the topography to avoid excessive pressure gradient errors to appear. Thus the real Oslofjord topography differs from the model topography. The effect is to lessen the gradient of steep slopes, for instance close to the coastline and at shelf breaks of the deeper basins. This should be kept in mind when comparing model results and observations.

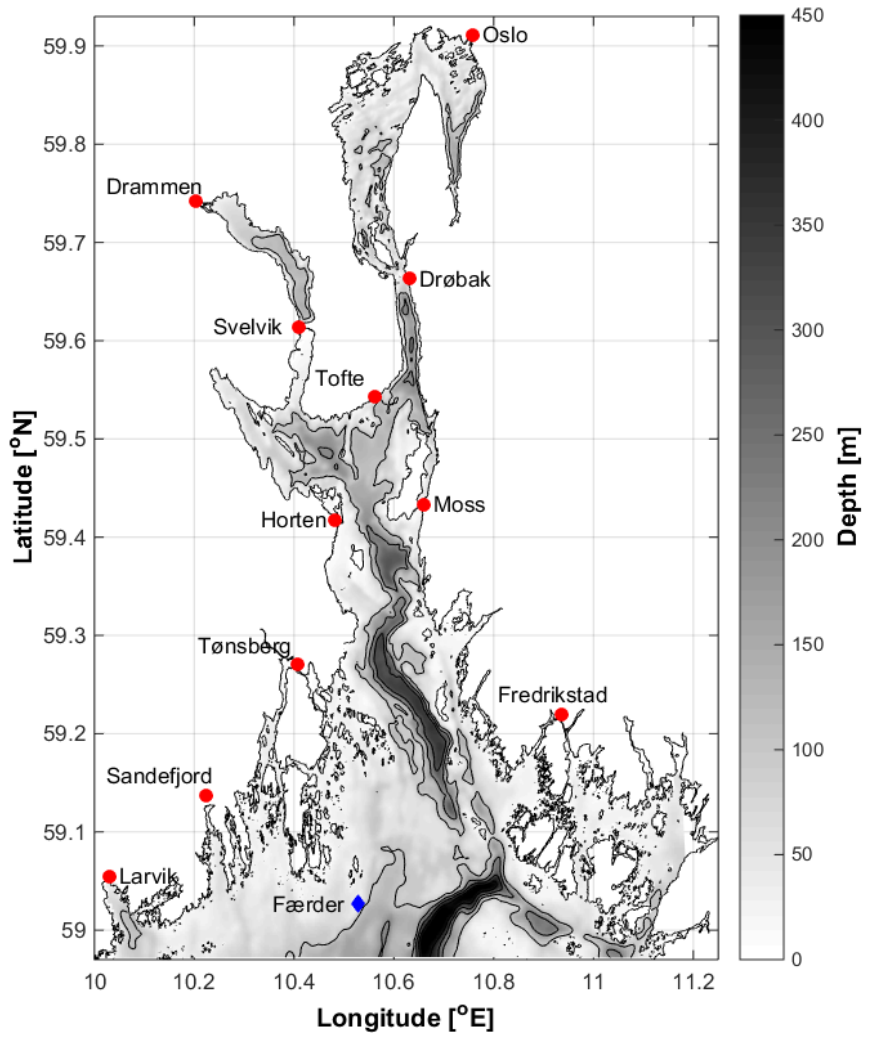


Figure 1: Displayed is the area covered by the Oslofjord and the FjordOs model. The red dots show the location of some major and minor cities and villages along the coast, and which are mentioned in the text. The blue diamond indicates the position of the Færder Lighthouse close to the model's southern boundary.

### 3 Observations

The relevant observed data in the area of interest are scattered in both time and space (Fig. 2). Observations over longer time period includes three stations measuring sea level (Viker, Oscarsborg, and Oslo), one bottom-mounted doppler measuring currents in two depth levels (Slagentangen), and one device measuring sea temperature (Scanmar AS). More occasional observations includes CTD measurements, current measurements, ferrybox, some drifter experiments, and water temperature at a few selected beaches during the summer.

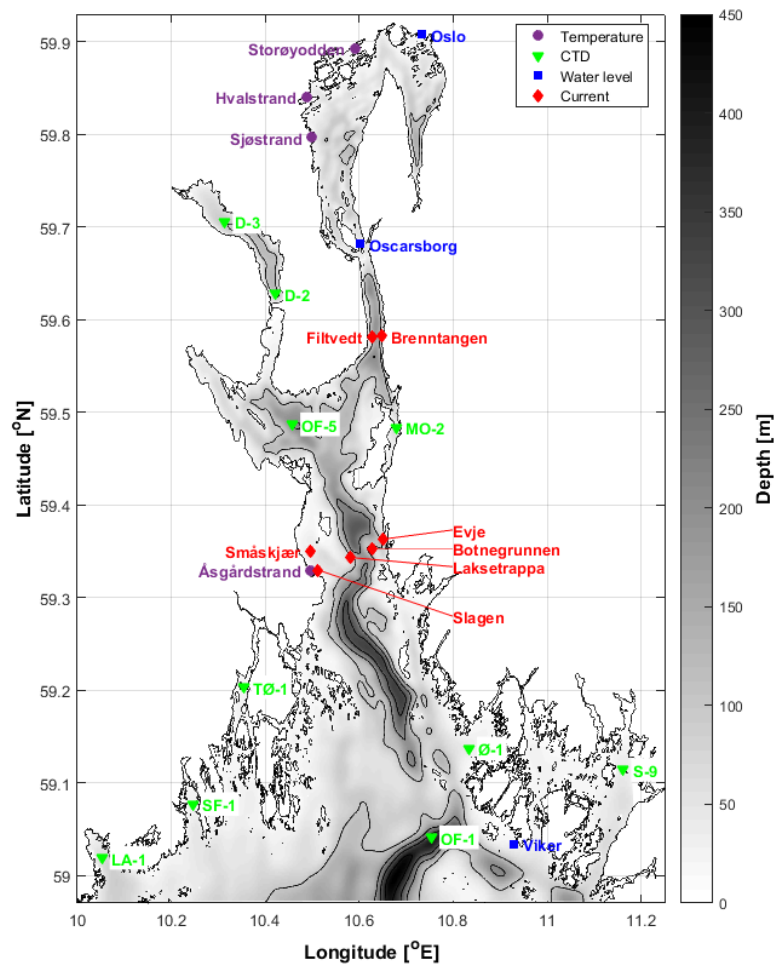


Figure 2: Positions for observations are marked.

### **3.1 Water level**

The Norwegian Mapping Authority has three permanent stations measuring sea level in the area of interest (Fig. 2). The station at Viker is placed close to the open boundary of the model area. The station at Oscarsborg is placed halfway in the Inner Oslofjord, and the station at Oslo is placed in the innermost part of the fjord.

### **3.2 Currents**

#### **3.2.1 Currents in two cross sections**

In the period from Monday 15th to Thursday 18th of September 2014 altogether seven rigs with instruments was deployed at seven positions in Oslofjorden (Tab. 1 and Fig. 2). In the period from Monday 24th to Wednesday 16th of November the seven rigs with instruments were recovered. All but one rig had profiling current meters, while the last rig had TinyTag temperature loggers deployed at seven different depths between 20 and 120 m. At one station a single point current meter was deployed just below the profiling current meter.

The rigs were deployed as a part of a project conducted by Statnett, NIVA, Akvaplan NIVA, and the University of Oslo. The research vessel F/F Trygve Braarud was used during deployment and recovery of the rigs. Details on the applied rigs and corresponding instruments can be found in *Staalstrøm and Ghaffari (2015)*.

The strongest currents were found where the fjord is relatively narrow, in the Drøbak Sound at the stations Filtvedt (Km1) and Brenntangen (Kn2). The stronger current in the more narrow part of the fjord can be explained by a stronger tidal signal due to the fjord geometry. In both the two transects across the fjord, it was the shallowest stations that had the highest current velocities. This can be explained by the fact that the horizontal pressure gradient has a tendency to decrease with depth.

Table 1: Target positions (WGS84) of the instrument rigs. Depths at the stations are from the Statnett terrain model.

Station	Name	Latitude	Longitude	Depth	Instruments
		[°N]	[°E]	[m]	
Kp11.2	Småskjær (Ri1)	59.350124	10.497661	20	Aquadopp600 AQP1531 Transducer LRT2
Kp5.7	Laksetrappa (Ri1)	59.343452	10.581023	75	Aquadopp400 AQP4689 Transducer LRT3 Aanderaa Seaguard
Kp2.6	Botnegrunden (Rm1)	59.352375	10.626822	96	Continental WAV6117 Transducer LRT4
Kp0.7	Evje (Rn1)	59.363182	10.653576	64	Aquadopp400 AQP2931 Transducer LRT5
Kn2	Brenntangen	59.581803	10.646087	54	Aquadopp400 AQP5608 Transducer LRT6
Km1	Filtvedt (current)	59.582064	10.627372	153	Continental CNL6037 Transducer 207-2
Km2	Filtvedt (temperature)	59.580778	10.626239	125	7 TinyTags UIO1-7 Transducer 203-2

### 3.2.2 Currents at Slagentangen

Using a bottom-mounted Doppler, Exxonmobil has measured the currents in two depths since 1997. The device is placed 50-80 meters northwest of Turning Dolphin at the Slagen Refinery (Fig. 2 and 3). Note that Bliksekilen nature reserve is located west of Slagen Refinery, which is a shallow water area with rare flora and fauna.

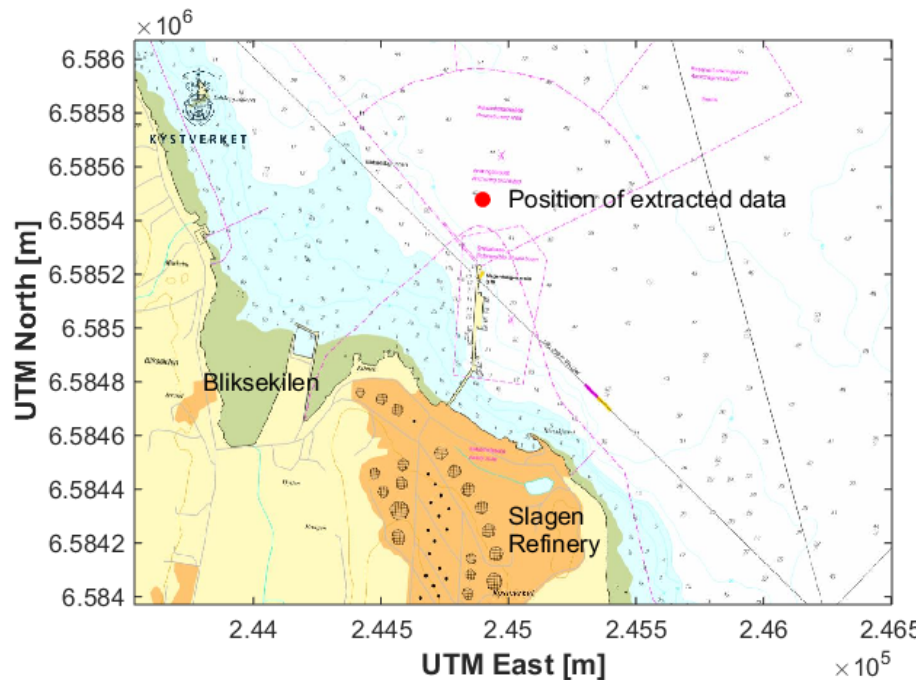


Figure 3: Map of Slagen Refinery. The red dot marks the position corresponding to the extracted simulated data. Source: Norwegian Coastal Administration

Table 2: The coordinates and number of measurements at the positions of the CTD measurements taken between April 2014 and December 2015 in the model area. Source: NIVA

Tag	Station	Latitude	Longitude	Number of measurements	
		[°N]	[°E]	2014	2015
D-2	Inner Drammensfjord	59.6280	10.4210	5	7
D-3	Solumstrand	59.7060	10.3140	5	6
LA-1	Larviksfjord	59.0190	10.0520	5	7
MO-2	Kippenes	59.4840	10.6780	5	7
OF-1	Torbjørnskjær	59.0410	10.7540	5	7
OF-5	Breiangen	59.4870	10.4580	5	7
S-9	Haslau, Singlefjord	59.1140	11.1620	7	10
SF-1	Sandefjord	59.0770	10.2460	5	7
TØ-1	Vestfjord	59.2030	10.3550	5	7
Ø-1	Leira. Vesterelva	59.1370	10.8340	7	10

### 3.3 Hydrography

#### 3.3.1 CTD measurements

In order to monitor the eutrophication state of the outer Oslofjord and the Drammensfjord, measurements are taken at selected positions in a monitoring program financed by Fagrådet for Ytre Oslofjord. The measurements include profiles of temperature and salinity with CTD as well as water quality parameters, and are available through a web portal<sup>1</sup>. Between April 2014 and December 2015 CTD profiles was measured 12 times. Profiles are typically taken in January, February, June, July, August, September and November. The data coverage in the monitoring program is lacking in spring and early summer. A selection of the CTD stations in the program are listed in Table 2 and plotted as green triangles in Fig. 2.

#### 3.3.2 Water temperature near Åsgårdstrand

Hourly temperature measurements at one meter depth over the last 10 years have been measured by Scanmar AS located three kilometres south of Åsgårdstrand. The device has

---

<sup>1</sup><http://www.aquamonitor.no/ytreoslofjord/>

an accuracy of  $\pm 0.15^{\circ}\text{C}$  in the range from -5 to  $+30^{\circ}\text{C}$ . Note that 2014 had a warmer summer followed by a warm winter resulting in higher maximum and lower minimum than 2015 (Fig. 4).

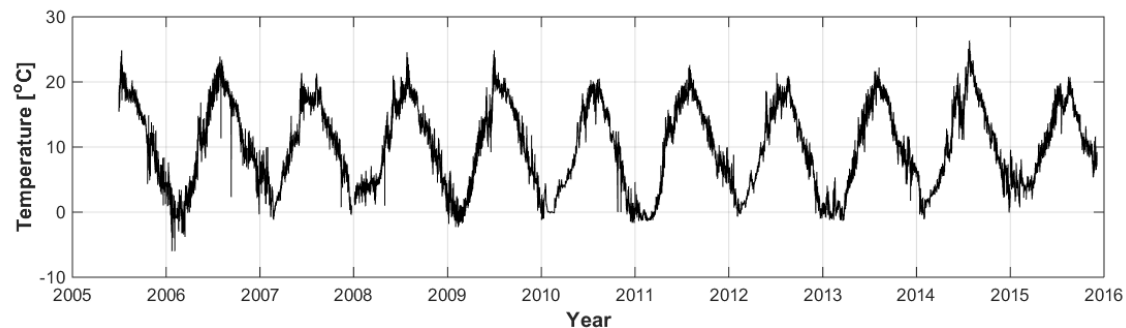


Figure 4: Observed temperature measured by Scanmar AS

### 3.3.3 Water temperature in the Inner Oslofjord

Temperature measurements at three beaches in the Inner Oslofjord (Fig. 5) are performed in a cooperation between Asker and Bærum kommune, and Finnerud Elektronikk. The digital thermometers (Maxim Integrated DS18B20) have an accuracy of  $\pm 0.5^{\circ}\text{C}$  and are placed 40 cm beneath the water surface in positions where the water depths are several meters. Temperatures are measured every three hours from 09:00 to 18:00 during the summer months.

The trends of the observed temperatures at the three beaches are similar, but the temperature is generally lower at the southern beach, Sjøstrand, than at the northern beach, Storøyoddern (Fig. 6). In 2014 there were two local maximums during July, and the maximum observed temperatures in 2014 were higher than in both 2013 and 2015. The temperature increases 1-3 degrees during the day and decreases during the night.

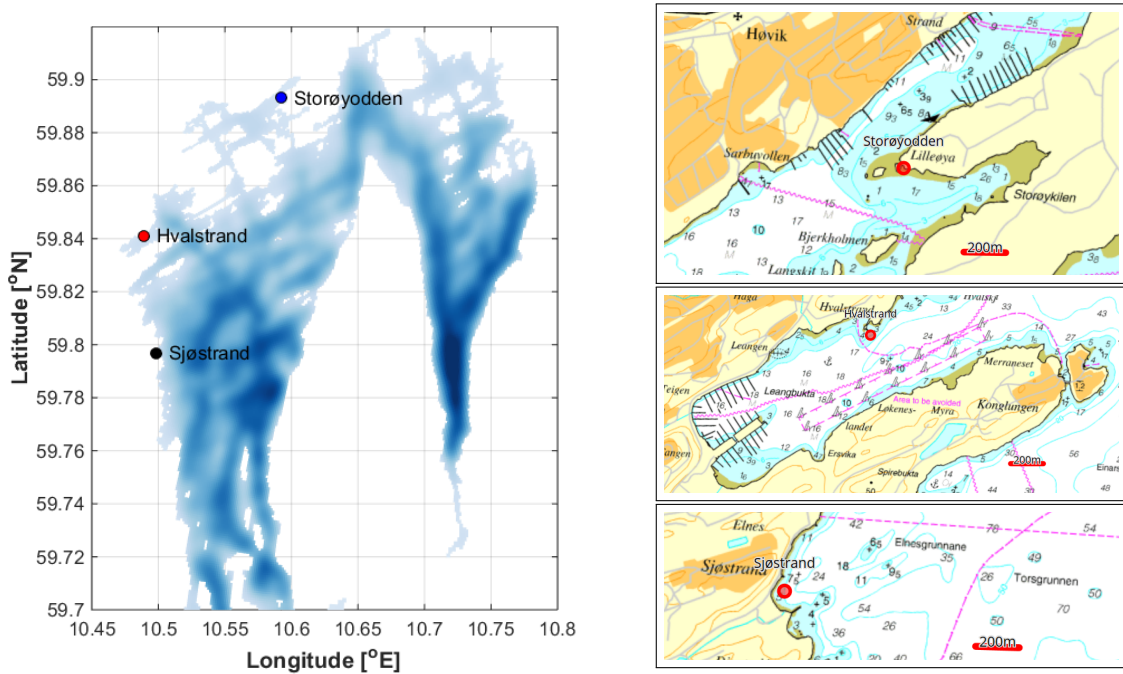


Figure 5: The positions at three beaches in the Inner Oslofjord where the temperature measurements are performed

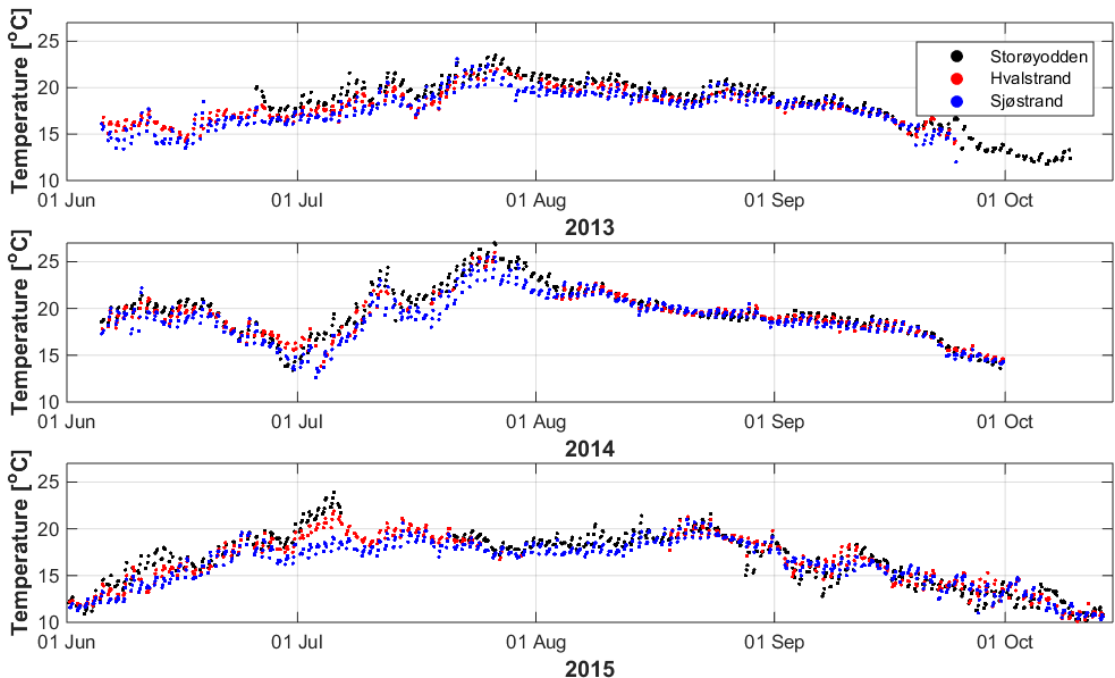


Figure 6: Observed temperature at three beaches in the Inner Oslofjord

### 3.4 Drifters and oil drift

We have observations of drift from release of surface drifters during two cruises in the Oslofjord, and from the oil spill during the grounding of the cargo ship Godafoss.

#### 3.4.1 Godafoss oil spill

The containership Godafoss ran aground at the Kværnskjærgrunnen rock in Løperen, between the islands of Asmaløy and Kirkøy in Hvaler municipality in southeastern Norway, on Thursday the 17th of February 2011 at 19:52 local time. One of the effects of this grounding was an acute release of oil from the ship, which drifted westward from the accident site. The oil slick has been observed from aeroplane by Kystverket, and the sites where stranded oil has been observed, are also registered (see Figure 7).

At the time of the grounding, the weather in the area was nice, clear skies and temperatures around -3°C. Observations of wind from Strømtangen lighthouse (15 km away from the grounding site) indicate 6-7 m/s winds from the north-east.

#### 3.4.2 Surface drifters

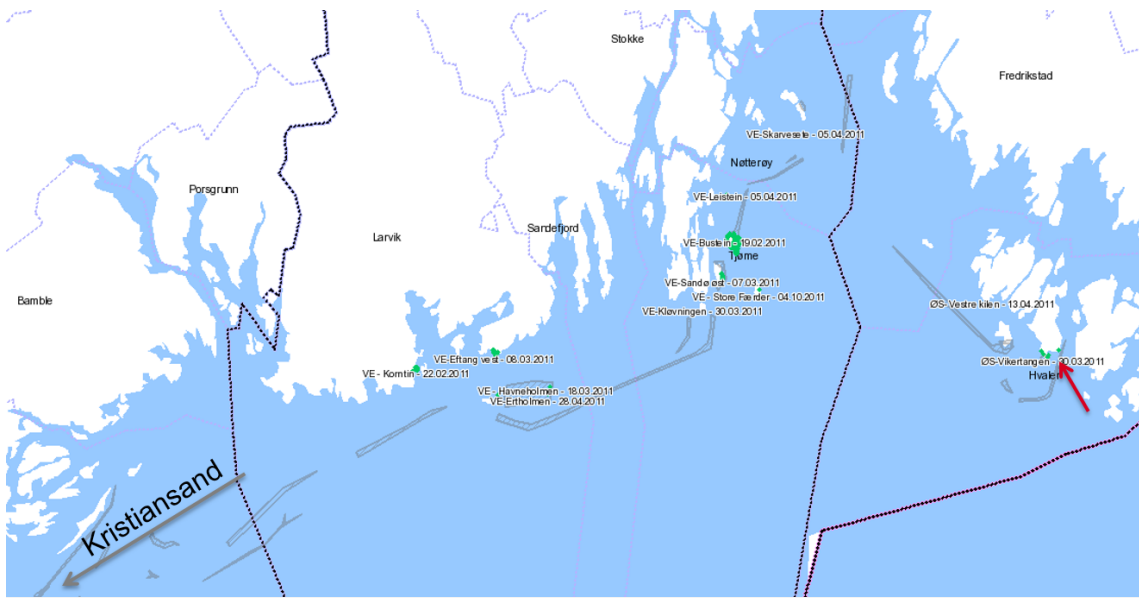


Figure 7: Observed oil spill from the Godafoss accident. The red arrow on the right hand side of the figure indicate the position of Kvaernskjærgrunnen, where the grounding happened, and from where the oil was released on the 17th of February 2011 at 19:52 LT. The grey areas are oil slicks observed from aircraft and the green areas indicate stranded oil. The text at the green areas in the figure also specify the name of the locations where oil has been observed, and when it was observed in those locations.

During a two cruises in the Oslofjord, we released a total number of 15 surface drifters (see Figure 8). Two were released during a cruise in September 2014, and the remaining 13 was released in a cruise in September 2015 (Figure 9). The second cruise, and the drifter type, is documented in *Hjelmervik et al.* (2016). The focus area of the drifter campaigns is the Breiangen area, and the area between Horten and Moss.



Figure 8: The "home-made" drifters used in this study. Depicted in the panel to the left when they are on board the research vessel (R/V) Trygve Braarud, and in the right hand panel after they have been deployed.

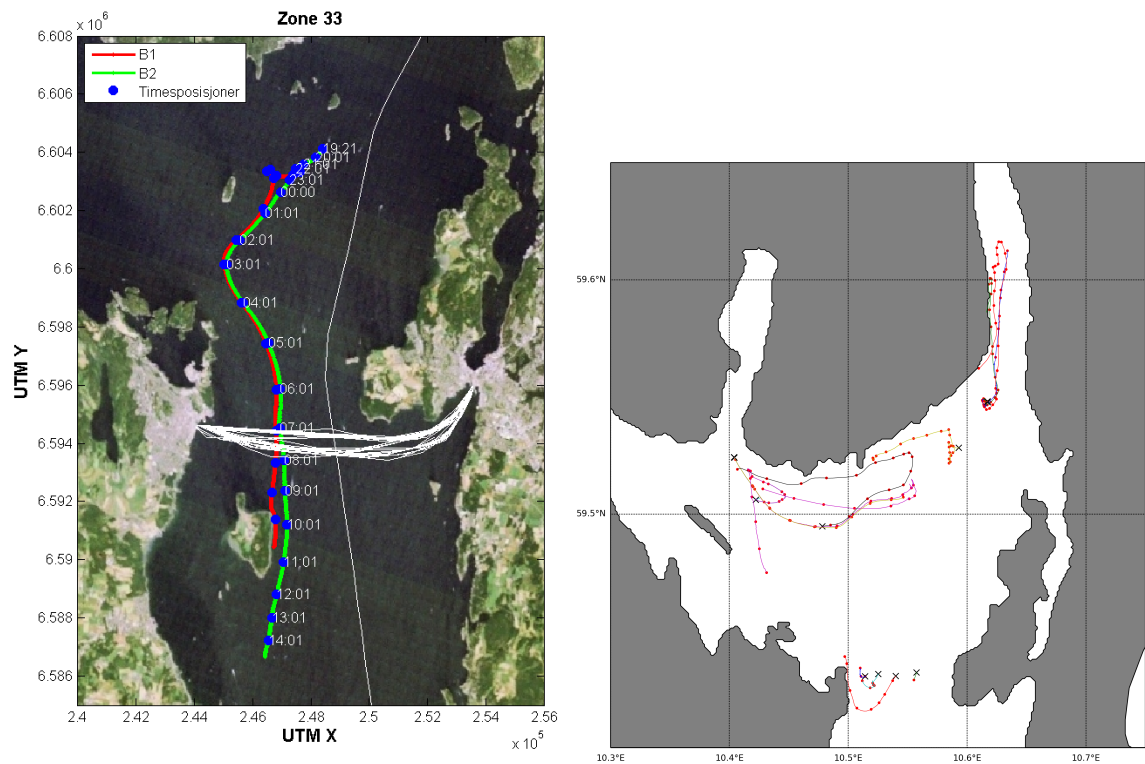


Figure 9: The tracks of the drifters. In the left panel is the two drifters released in September 2014, and in the right panel the drifters released during the cruise in September 2015.

## 4 Evaluation

### 4.1 Water level and tide

Time series from the three permanent stations measuring water level have been analysed and compared with simulated time series of water level extracted from locations near the three permanent stations. Both simulated and observed time series of water level are analysed using `t_tide` (*Pawlacz et al.*, 2002) in order to extract the tidal components. The same period in time is applied for both the simulations and the observations (April 2014 to December 2015).

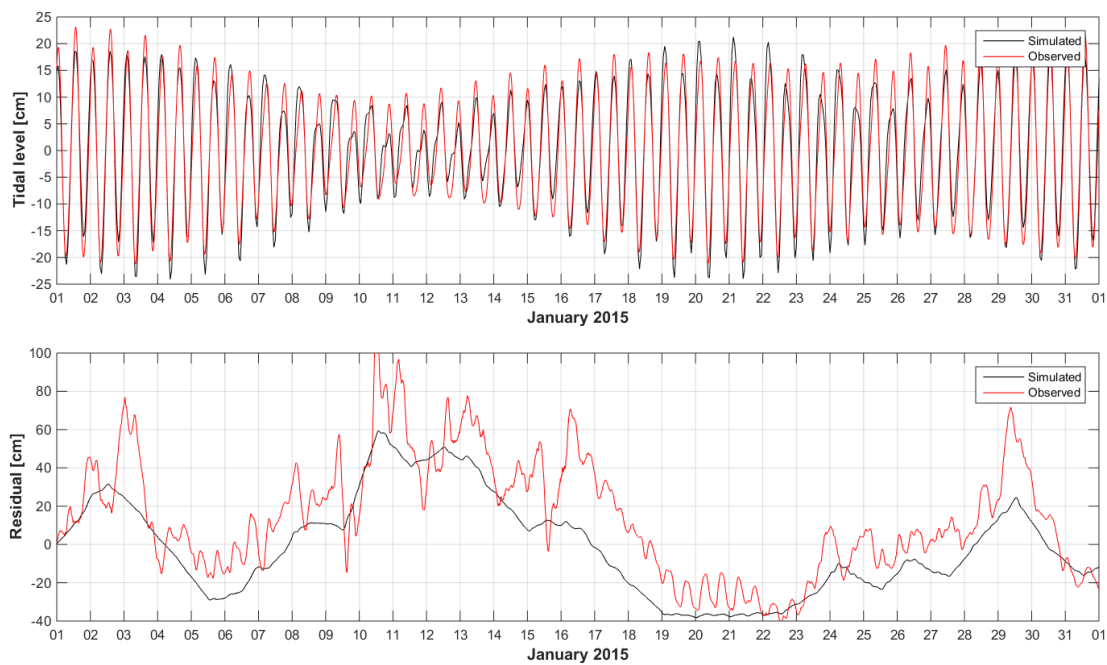


Figure 10: Simulated (black) and observed (red) time series of tides (upper) and residual (lower) at Oscarsborg. Here the tidal elevation includes only the eleven components included in the tidal forcing. The residual includes the total water level minus the tidal elevation.

Eleven tidal components are included in the model at the southern open boundary using their corresponding amplitudes and phases for both depth integrated currents and water level (*Røed et al.*, 2016). The time series of tidal components included in the tidal forcing are in fairly good agreement (Fig. 10,upper, and Tab.3). In addition to the tidal components included in the tidal forcing, more tidal components are present in the time series (Fig. 11). Tidal components with periods of approximately one year (SA) and half

a year (SSA) respectively are present in both the observations and the simulations (Tab.3). In addition, the observations have more components with shorter periods which are not included in the tidal forcing and thereby not present in the simulations. This is consistent with the frequency series of the Fourier transformed water level (Fig. 12).

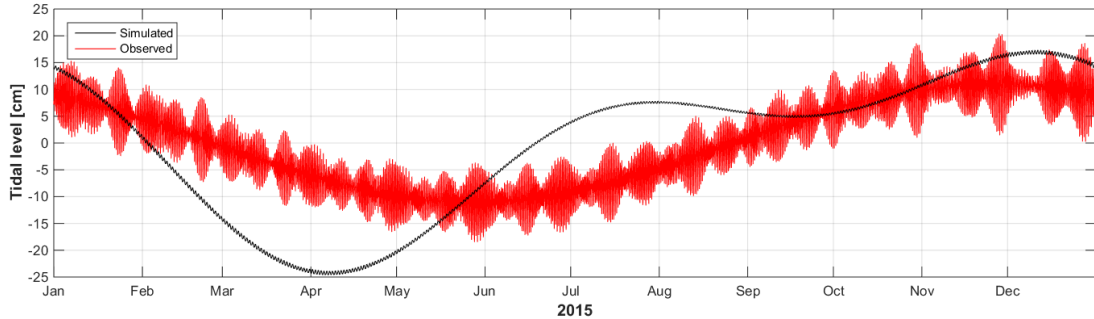


Figure 11: Time series at Oscarsborg of the tidal components not included in the tidal tidal forcing.

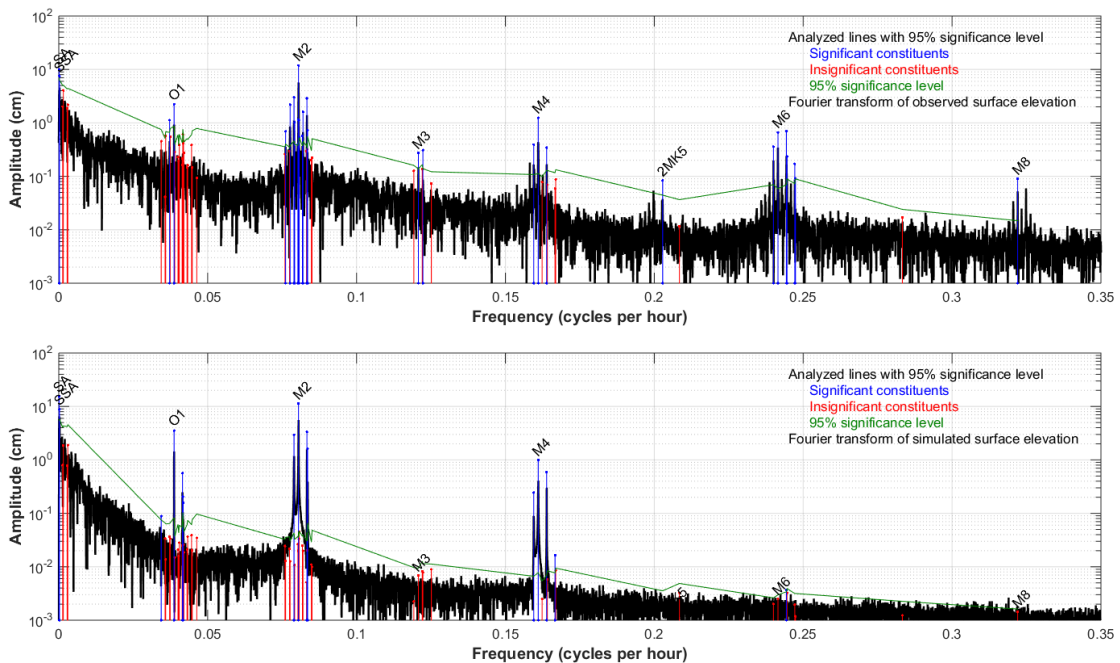


Figure 12: Frequency series of Fourier transformed observed (upper) and simulated (lower) water levels at Oscarsborg

The amplitude of  $M_2$  increases from south to north in the Inner Oslofjord both in the simulations and the observations (Fig. 13 and Tab. 3). The lowest  $M_2$  amplitude in the area of interest, is in the Drammensfjord north of the threshold in Svelvik. The  $M_2$  phase has a sudden increase at the thresholds of Svelvik and Drøbak (Fig. 13). The same yields for the majority of the other relevant tidal components.

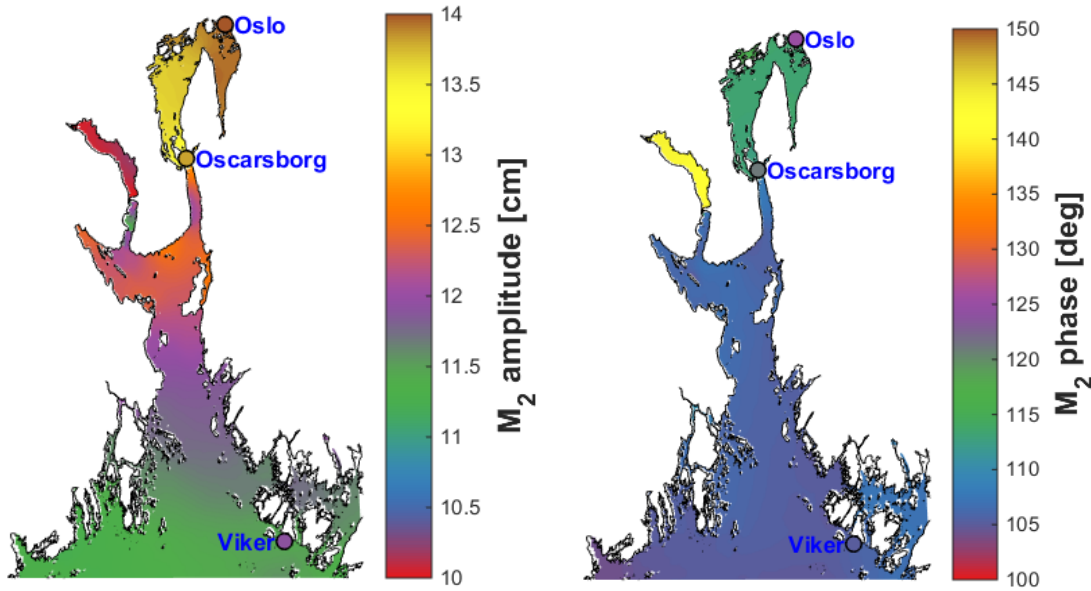


Figure 13: Simulated field of  $M_2$  amplitude (left) and phase (right). The corresponding observed values for  $M_2$  amplitude and phase are marked with circles at Viker, Oscarsborg, and Oslo.

Table 3: Simulated and observed tidal amplitude and phase for selected tidal components.

Comp.	Period [h]	sim/ obs	Viker		Oscarsborg		Oslo		Included in tidal forcing
			amp. [cm]	phase. [deg]	amp. [cm]	phase. [deg]	amp. [cm]	phase. [deg]	
SA	8764	sim	15.5	284	15.6	286	15.4	286	no
		obs	10.0	319	11	322	11.4	324	
SSA	4382	sim	8.8	197	9.2	200	9.4	200	no
		obs	7.5	188	8.0	189	8.2	190	
K2	11.9672	sim	1.6	10	2.0	13	2.1	15	yes
		obs	0.7	45	0.8	66	0.9	66	
S2	12.0000	sim	3.3	64	3.9	69	4.2	70	yes
		obs	2.9	46	3.3	65	3.5	69	
M2	12.4206	sim	11.5	105	13.2	112	13.9	114	yes
		obs	11.9	105	13.8	121	14.4	125	
N2	12.6584	sim	3.0	69	3.5	75	3.7	76	yes
		obs	3.0	60	3.4	76	3.6	80	
K1	23.9345	sim	0.2	187	0.1	175	0.2	157	yes
		obs	0.4	127	0.7	130	0.8	130	
P1	24.0659	sim	0.6	322	0.6	334	0.7	342	yes
		obs	0.2	129	0.3	102	0.4	97	
O1	25.8193	sim	3.5	337	3.8	339	3.8	339	yes
		obs	2.2	277	2.3	281	2.4	282	
Q1	26.8684	sim	0.0	231	0.0	216	0.1	215	no
		obs	1.1	190	1.2	198	1.3	200	
MN4	6.2692	sim	0.2	5	0.5	32	0.6	35	yes
		obs	0.4	249	0.6	289	0.7	297	
M4	6.2103	sim	1.0	355	1.9	18	2.5	23	yes
		obs	1.2	281	1.8	324	2.3	332	
MS4	6.1033	sim	0.6	80	1.2	107	1.6	111	yes
		obs	0.3	360	0.5	44	0.7	56	

## 4.2 Currents

### 4.2.1 Currents in two cross sections

Current measurements were performed in two cross sections. Here the model results are evaluated using the measurements at the northern cross section, Brenntangen-Filtvedt. The results are similar at the southern cross section.

The observed and simulated currents at Filtvedt and Brenntangen are of the same magnitude in strength, but the flow pattern differs. Figure 14 shows the observed and simulated currents at Filtvedt as an example. The observed currents at Brenntangen is similar in strength, but the peaks in current strength do not occur at the same time. The observations are dominated by noise in the upper 35-40 meters. Only depths larger than 40 meters are therefore included in the comparison.

Note that the 3D current field is complex, the currents vary horizontally, vertically and with time. Figure 15 shows the simulated currents at three different depths. In general, the currents in the upper layer are stronger than further down. In the upper layers the currents are towards north, at 40 meters depth the currents towards south, and at 100 meters depth towards north. Because of the complex flow pattern, the currents at a given coordinates cannot be taken as representative for the whole area. At 100 meters depth the currents at Filtvedt are weak and towards south even though the currents at 100 meters depth is generally stronger and towards north. At 40 meters depth the currents at Brenntangen is weaker than in the rest of the cross section. Note that the depth at Brenntangen is only 58 meters in the observations while in the depth is 46 meters at the corresponding point in the simulations.

The tides are evident in the observed and simulated currents at all observation points. Both simulated and observed time series of the currents at the seven observation points are analyzed using *t\_tide Pawlowicz et al. (2002)* in order to extract the tidal components for each depth. The same period in time is applied for both simulations and observations (mid-September to the end of November 2014). Figure 16 shows the tidal currents at Filtvedt. At Filtvedt the tidal impact in the observations occurs earlier at larger depths, but in the simulations the tidal impact occurs earlier at more shallow depths. This might be due to the flow pattern at the different depths and the fact that the flow pattern depends strongly on the bottom topography which is smoothed in the simulations. Note also that the calculations of the tides are based on only six weeks of data.

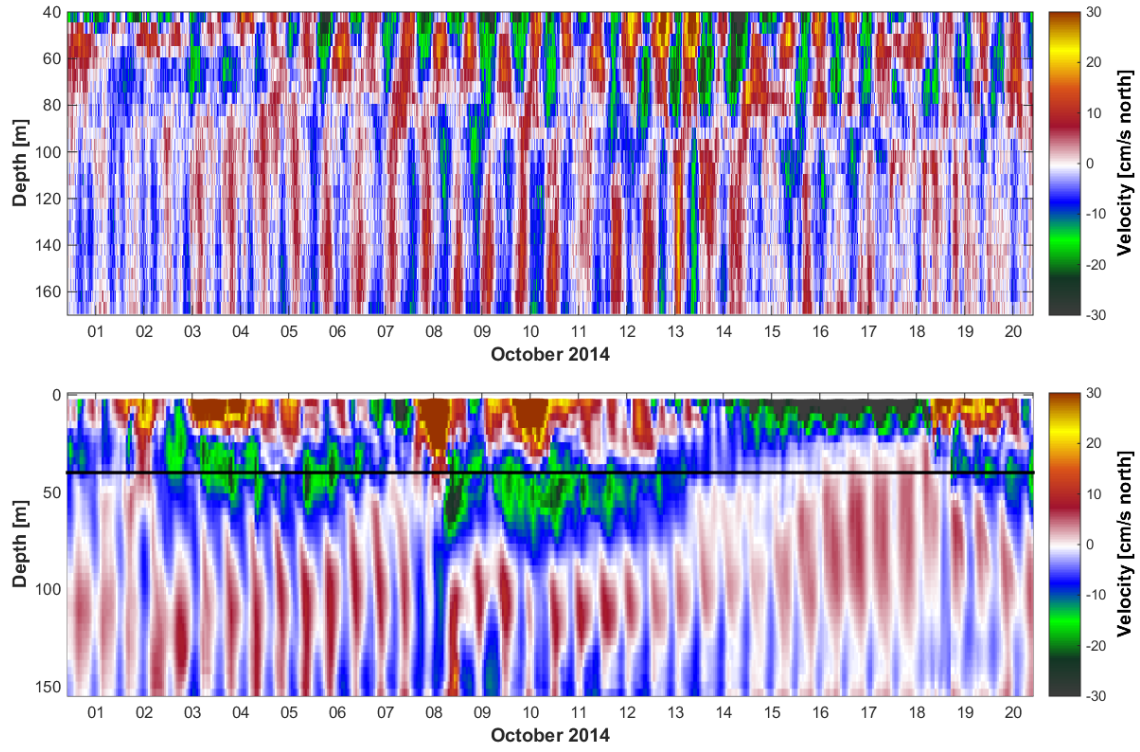


Figure 14: Observed (upper) and simulated (lower) currents at Filtvedt. Since the observations near the surface were dominated by noise, only depths larger than 40 meters are included in the upper plot.  $z = 40$  meters is marked with a black line in the lower plot. Note that the model depth is only 155 meters at the position the observations were performed.

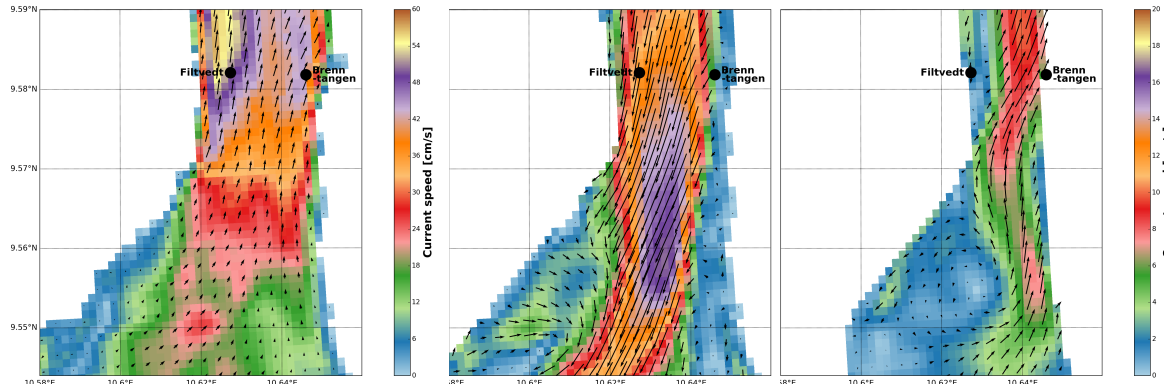


Figure 15: Simulated currents at 2 (left), 40, and 100 (right) meters depth at 10 October 2014 12:00. Note that the two plots to the right have the same colorbar.

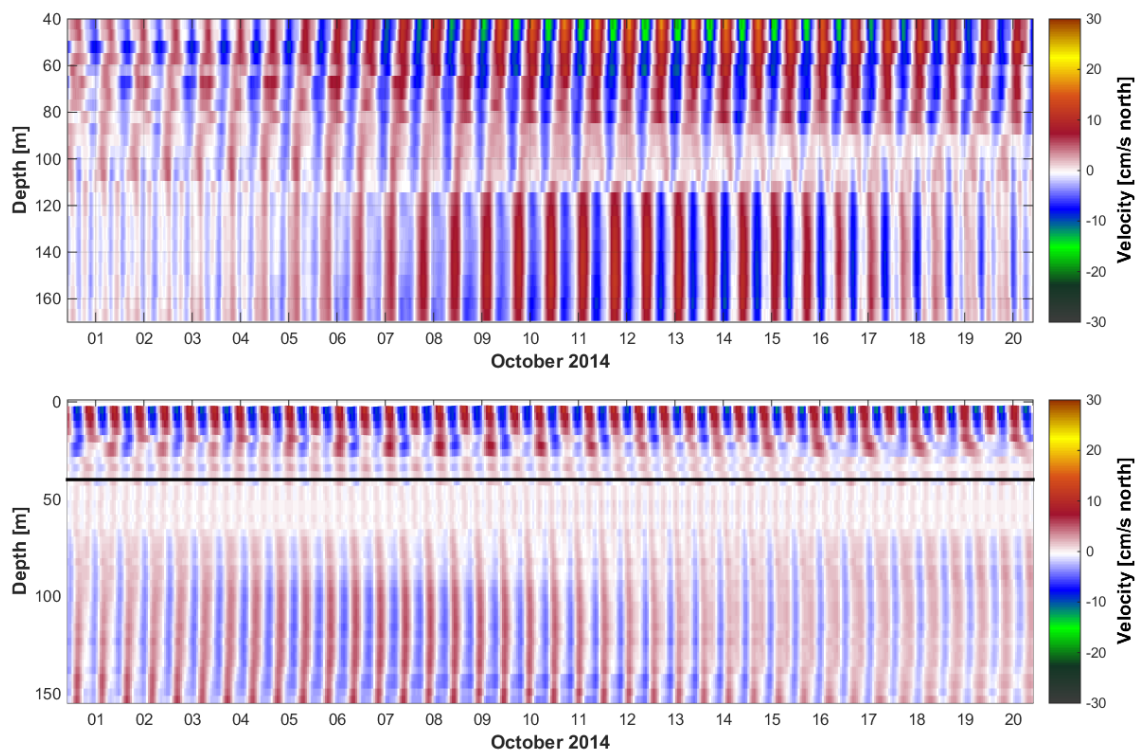


Figure 16: Observed (upper) and simulated (lower) tidal currents at Filtvedt.

## 4.2.2 Current at Slagentangen

The observed currents at Slagentangen are compared with simulated data from 1st October 2014 until 30th November 2015 at approximately the same location and depth (Fig. 3).

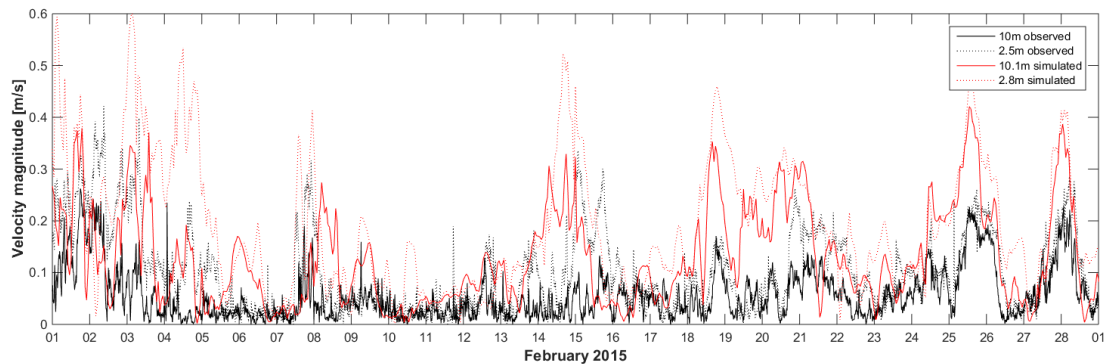


Figure 17: Timeseries of observed and simulated velocity magnitudes at Slagen.

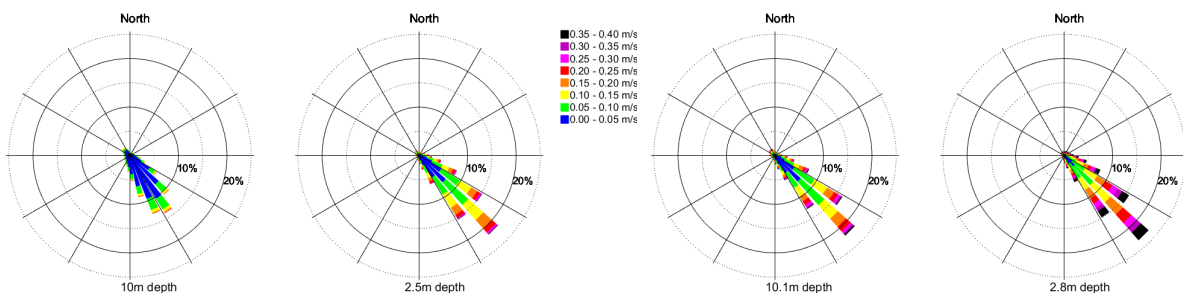


Figure 18: Current roses for observed (left) and simulated (right) velocity magnitude at the two depths from 1st of October 2014 to 1st of October 2015.

Time series reveal that the observed velocities varies and follows no striking pattern (Fig. 17). Current roses show that both the observed and the simulated velocities are stronger in the upper layer (Fig. 18). The simulated velocities are stronger than the observed velocities. This is in accordance with the probability density functions (Fig. 19). The yearly maximum observed velocities are approximately 0.4 and 0.6 m/s at 10 and 2.5 meters depth respectively (Tab. 4). During 2014 and 2015 maximum observed velocity at 2.5 meters depth was 0.55 m/s in southeast direction ( $143^{\circ}$ N) the 26th of March 2014. The velocity at 10 meters depth was 0.08 m/s ( $153^{\circ}$ N) at the time of maximum velocity at 2.5 meters depth indicating that the velocities are different in the two layers.

The mean directions are to the south east. At approximately 2.5 meters depth the mean directions are  $146^{\circ}$ N and  $139^{\circ}$ N for observed and simulated directions respectively

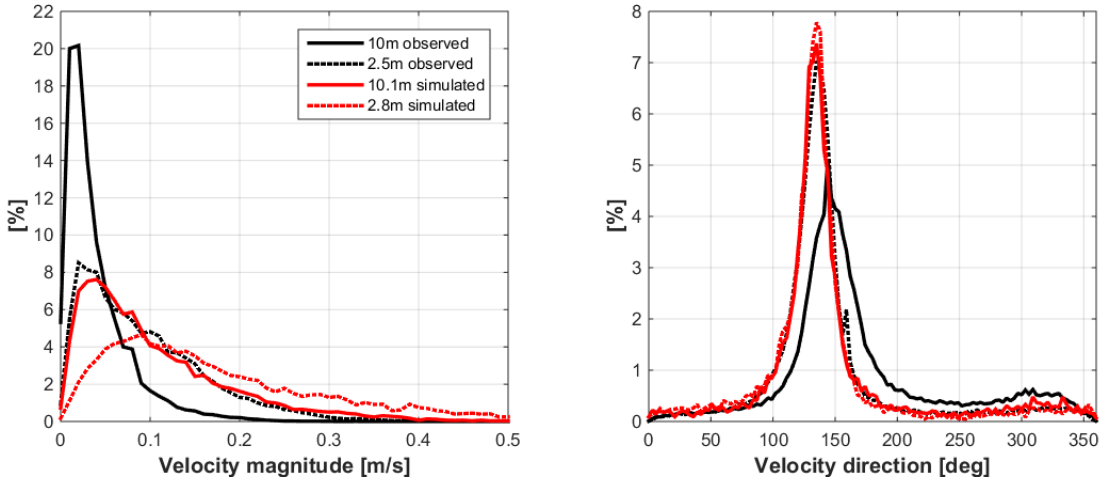


Figure 19: Probability density functions of velocities and directions at Slagen for 1st of October 2014 to 1st of October 2015. The bin width is 0.01 knots for velocity and 3 degrees for direction.

which is in fairly good agreement. At approximately 10 meters depth the observed mean direction shifts to  $170^{\circ}\text{N}$  while the simulated mean direction is  $148^{\circ}\text{N}$ . Testing with popcorn indicate that the preferred direction of the surface currents are towards Bliksekilen located west of the Slagen Refinery. This is not the case neither in the observations nor the simulations. The probability density functions reveals that the model captures the distribution of directions in the upper layer, but does not capture the change in direction between the two depths (Fig. 19). The standard deviations at 2.5 and 10 meters are 55 and 66 degrees respectively for the observed directions, and 56 and 61 for the simulated directions.

The time series scatter plots reveal that the correlation in time is not satisfying (Fig. 17 and 20). The model seem to have difficulties with capturing the right phenomena influencing the currents to the right time. This is a well known problem when it comes to forecasting currents. The QQ-plots also confirms that the simulated currents are stronger than the observed currents.

Table 4: Yearly maximum observed velocity at Slagen.

Year	Max. velocity at 10m depth			Max. velocity at 2.5m depth		
	Date	[m/s]	[deg]	Date	[m/s]	[deg]
2006	21 Jan 2006	0.42	139	31 Oct 2006	0.57	140
2007	14 Jan 2007	0.42	172	21 Aug 2007	1.03	359
2008	22 Mar 2008	0.36	149	19 Dec 2008	0.57	160
2009	17 Dec 2009	0.45	142	24 Mar 2009	0.56	139
2010	09 Nov 2010	0.41	138	09 Nov 2010	0.54	138
2011	01 Jan 2011	0.39	146	30 Mar 2011	0.62	185
2012	05 Dec 2012	0.39	138	29 May 2012	0.57	140
2013	10 Oct 2013	0.42	143	10 Oct 2013	0.49	144
2014	18 Apr 2014	0.44	147	26 Mar 2014	0.55	143
2015	24 Jan 2015	0.33	128	21 Mar 2015	0.55	141

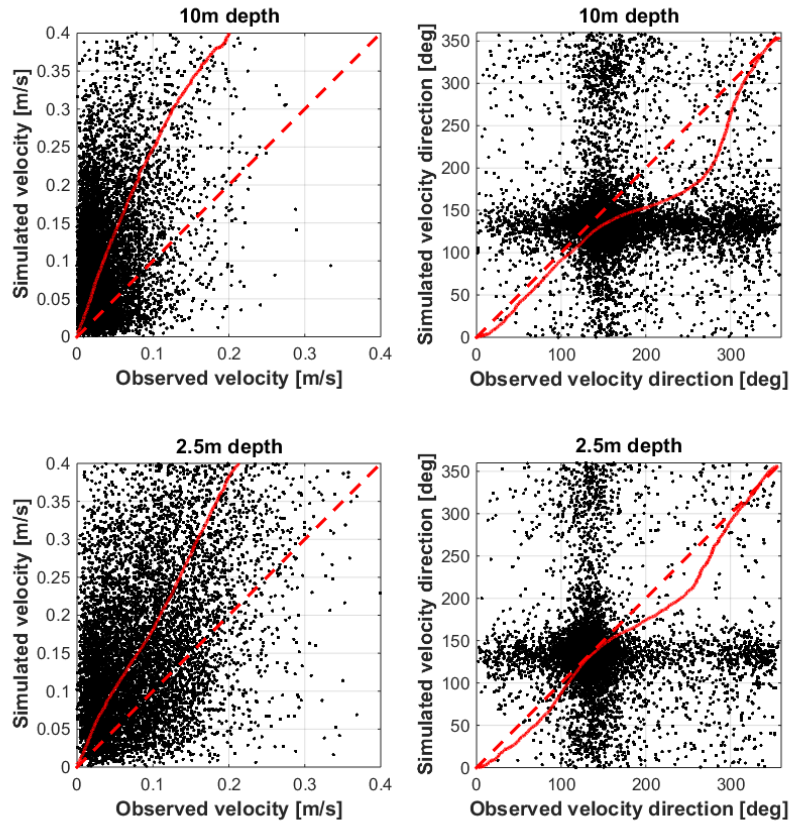


Figure 20: Combined QQ- and scatter plot of observed and simulated current at Slagen from 1st of October 2014 to 1st of October 2015.

## 4.3 Hydrography

### 4.3.1 CTD-measurements

Positions where CTD measurements are taken in the monitoring program for the Outer Oslofjord are listed in Table 2. Simulated temperature and salinity profiles at some of these stations are extracted from the model run. Comparison between simulated and observed profiles are shown in Figs. 21- 23, for the stations OF-1 in the outer part of the fjord, LA-1 in Larvikfjord and D-2 inside the Svelvik Sill in the inner Drammensfjord.

During the summer, the water in the upper layers are heated. The maximum surface temperature is observed towards the end of the summer. The profiles in the outer parts of the fjord indicate that the upper layer is too thin in the simulated data (Fig. 21). At larger depths, the water is too cold and the salinity is too high. This might indicate that the open boundary input and the representation of vertical mixing should be modified.

Some of the observations are taken from smaller fjord branches, such as in the Larviksfjord close to the open boundary in the outer part of the Oslofjord. In such shallow waters, observations reveal that the whole water column is heated during summer and cooled during winter, but the simulated temperature varies only in the upper 20 meters (Fig. 21).

The water masses below sill depth in the Drammensfjord are known to have very low vertical diffusivity leading to low oxygen conditions in the depth. Fig. 23 reveals that the vertical diffusivity in the same basin in the model is two high. In the model water with low salinity is mixed down all the way to the bottom.

To get a better idea of how the properties of the water masses varies with time, contour plots of salinity and temperature are made as a function of depth and time. Three of the stations in the monitoring program are chosen to describe how the salinity and temperature in different parts of the fjord system evolves through two seasons. Station D-3 outside Solumstrand in the inner Drammensfjord, station OF-5 in Breiangen and station OF-1 near Torbjørnskær close to the open boundary of the model domain, are chosen.

Observed salinity and temperature at the three chosen stations are shown in Figs. 24 and 25 respectively. If the salinity of the stations OF-5 and OF-1 are compared (middle and lower panel in Fig. 24) it can be seen that the variations at for instance 40 m depth in Breiangen follow the variations further out in the fjord, but is approximately 1 psu fresher. This indicate a relatively good water exchange in the outer part of the fjord system. The water masses below sill depth in the Drammensfjord is different. The salinity below 40 m depth is lower than at the same depth in Breiangen, and the salinity change very little with

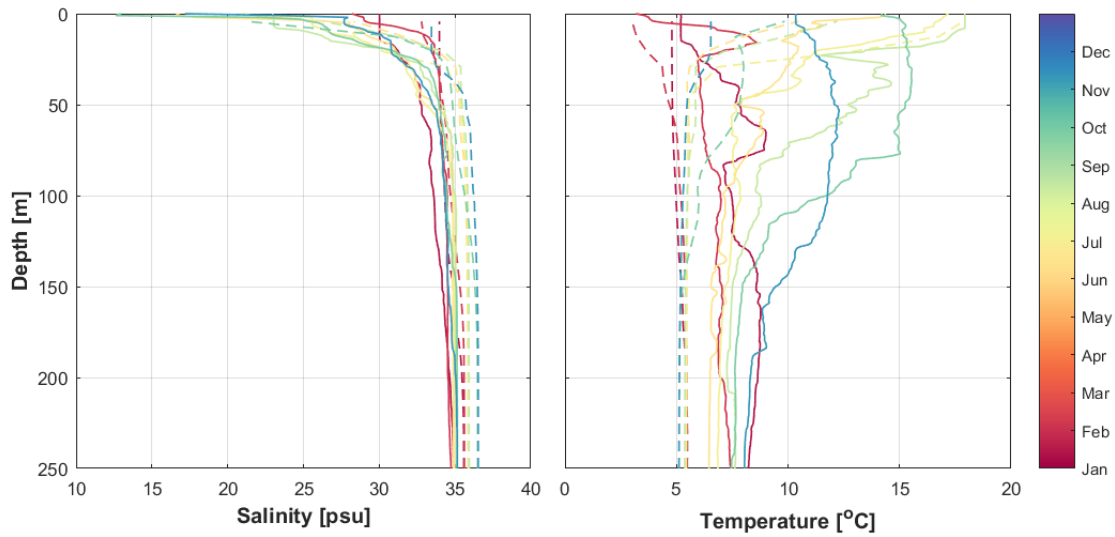


Figure 21: Observed (solid) and simulated (dashed) salinity and temperature profiles at station OF-1 Torbjørnskjær in the outer part of the Oslofjord. All profiles are from 2015.

time. These are clear signs of a stagnant water mass, and is expected given the shallow sill depth of only 12 m at Svelvik.

The seasonal temperature changes in the surface layer is slowly diffused down in the water masses in the outer part of the fjord system (middle and lower panel in Fig. 25). The temperature at 100 m depth has a seasonal change, but the maximum value is shifted in time, so the highest temperatures are found in the start of January at this depth. As seen in the upper panel in Fig. 25 the temperature variations in the surface layer in the Drammensfjord is prevented from penetrating further down than about 40 m depth due to the low vertical diffusivity.

Fig. 26 shows the salinity at the three chosen stations extracted from the model. The water exchange in the model between the two stations OF-5 and OF-1 is relatively good, and the variations at OF-1 follow the variations further out in the fjord. This was the same we saw from the observations. The salinity however is to high at mid depth and this can as mentioned above be due to wrong open boundary input or vertical diffusivity. The upper panel in Fig. 26 shows that the deep water masses in the Drammensfjord have a high salinity at model initialisation, but fresh water from the surface is quickly mixed down.

Fig. 27 shows the temperature at the three chosen stations extracted from the model. When the modelled temperature evolution in the outer part of the fjord system is compared with the observations, the vertical mixing seems to be too low, and the heating of the

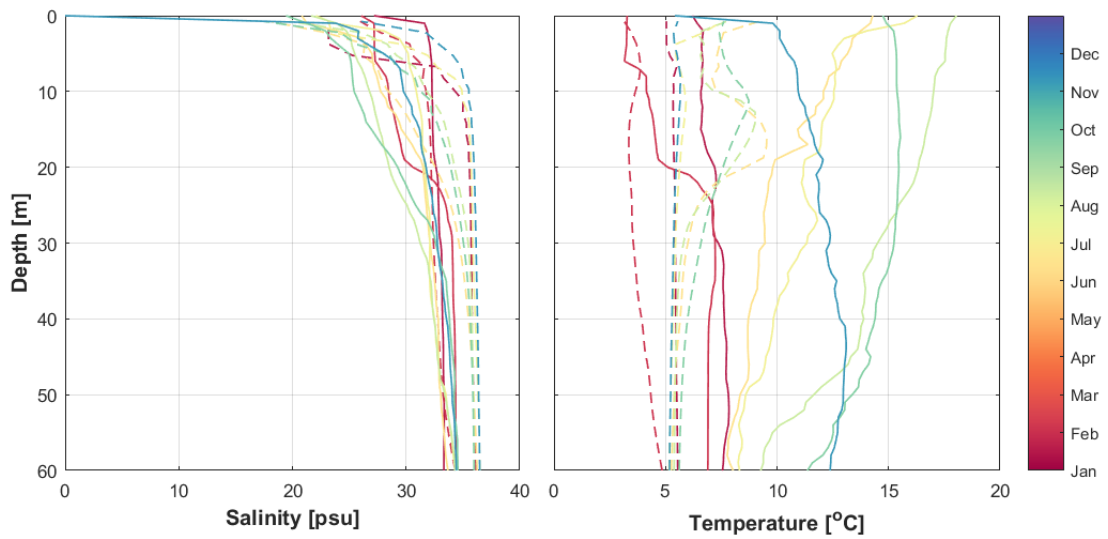


Figure 22: Observed (solid) and simulated (dashed) salinity and temperature profiles at station LA-1 Larviksfjord in a fjord branch in the outer part of the Oslofjord. All profiles are from 2015.

surface water during summer do not penetrate deep enough during the winter. While inside the Svelvik Sill the surface waters are mixed down too deep.

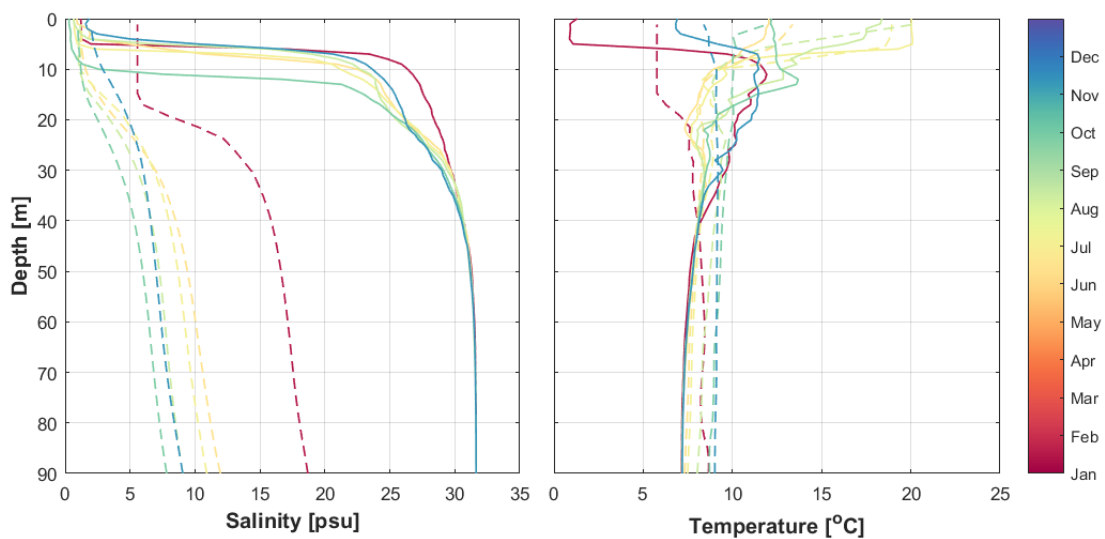


Figure 23: Observed (solid) and simulated (dashed) salinity and temperature profiles at station D-3 Solumstrand. All profiles are from 2015.

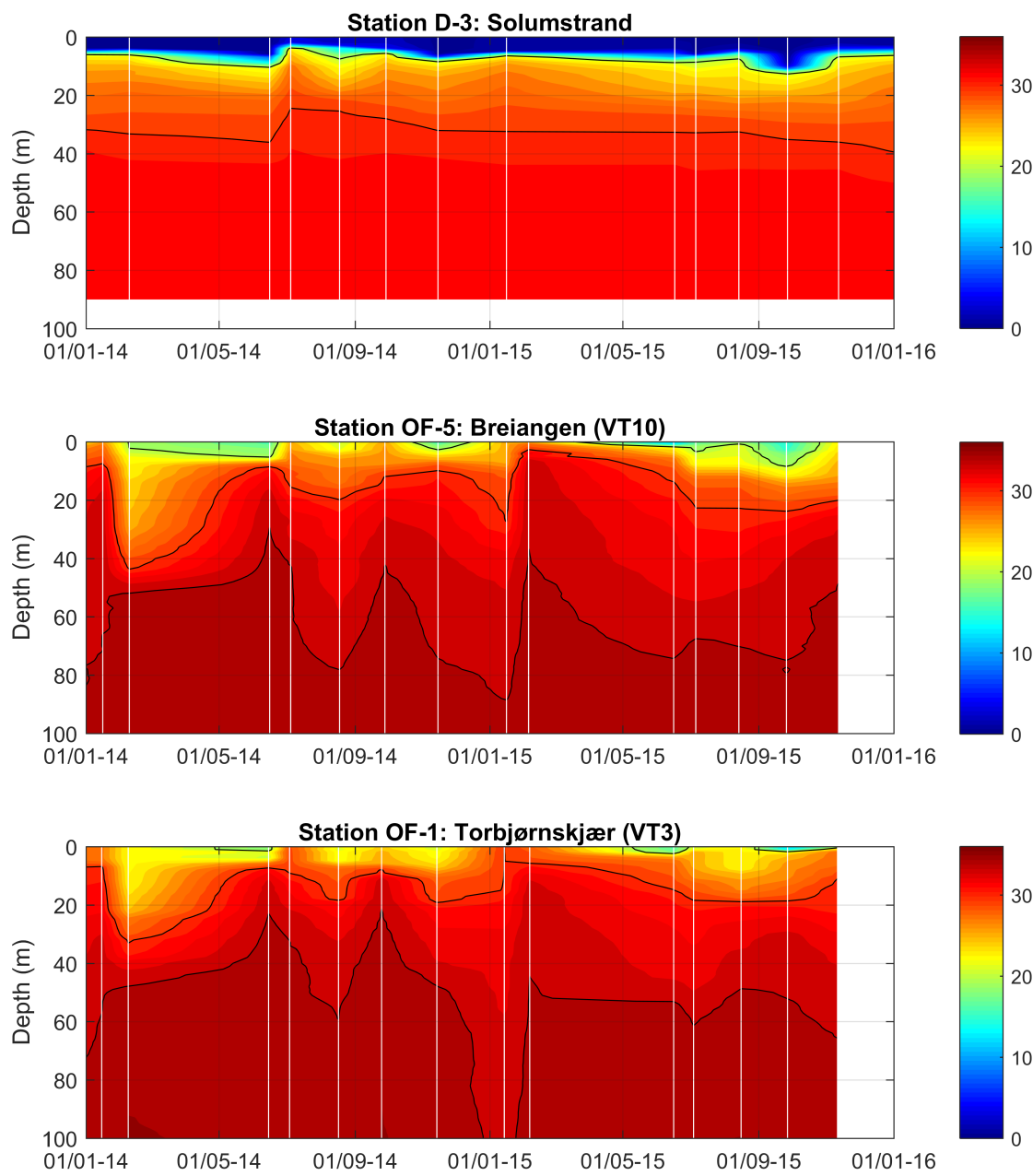


Figure 24: Observed salinity at three stations in the Oslofjord. Contour lines mark 20, 30, and 34 psu. The white vertical lines indicate the positions when CTD casts were taken.

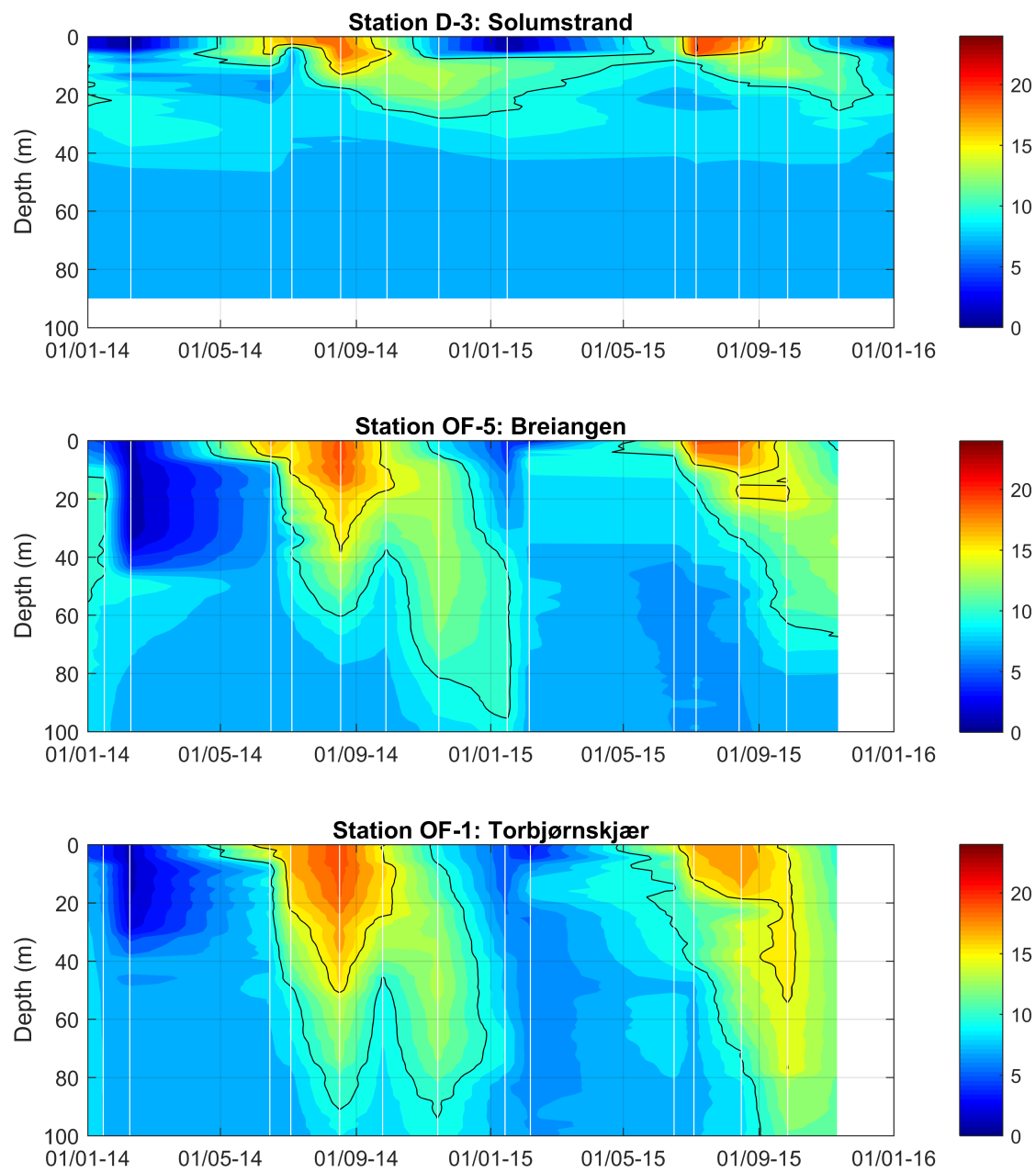


Figure 25: Observed temperature at three stations in the Oslofjord. Contour lines mark 5 and 10 °C. The white vertical lines indicate the positions when CTD casts were taken.

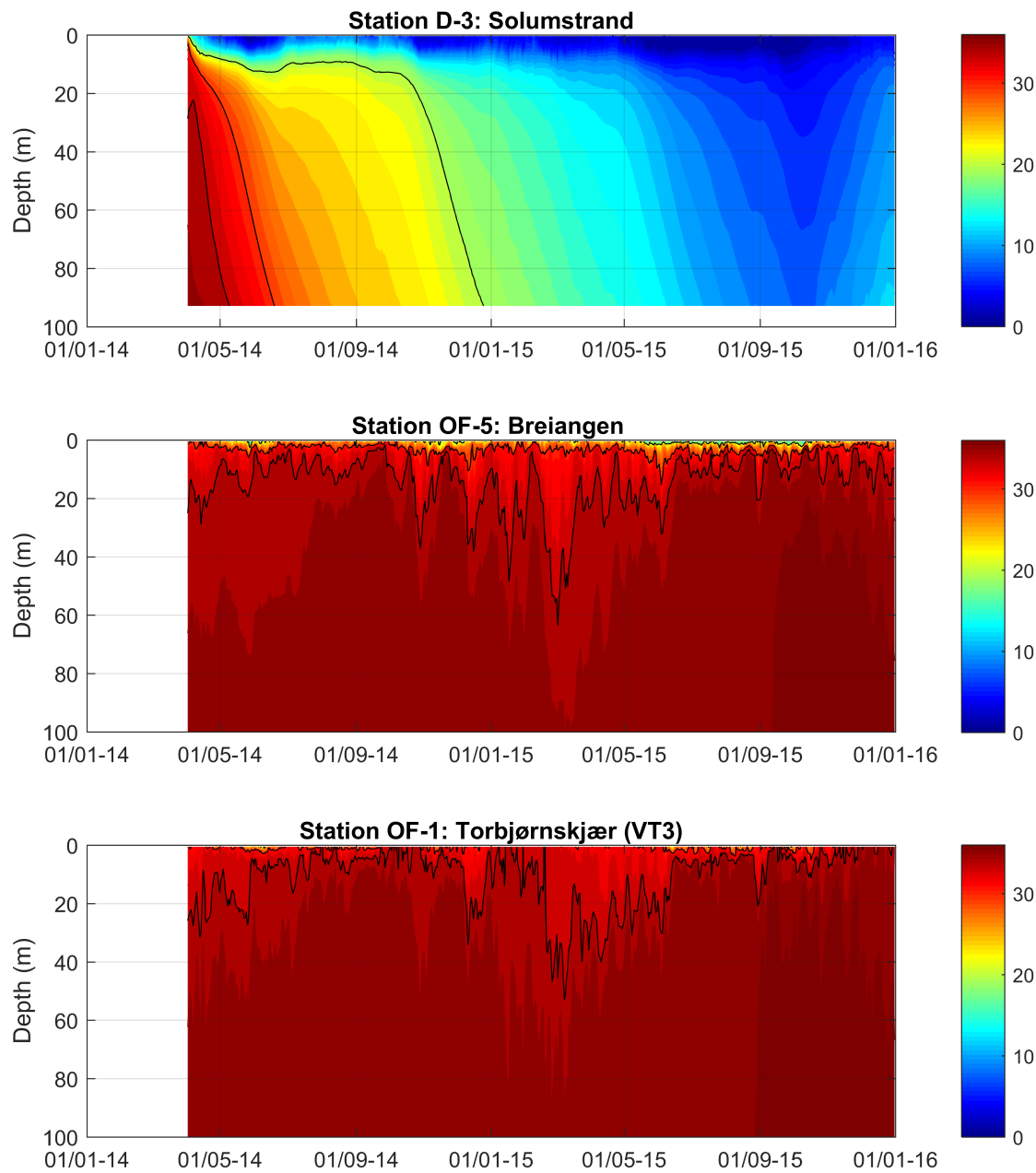


Figure 26: Modelled salinity at three stations in the Oslofjord. Contour lines mark 20, 30, and 34 psu.

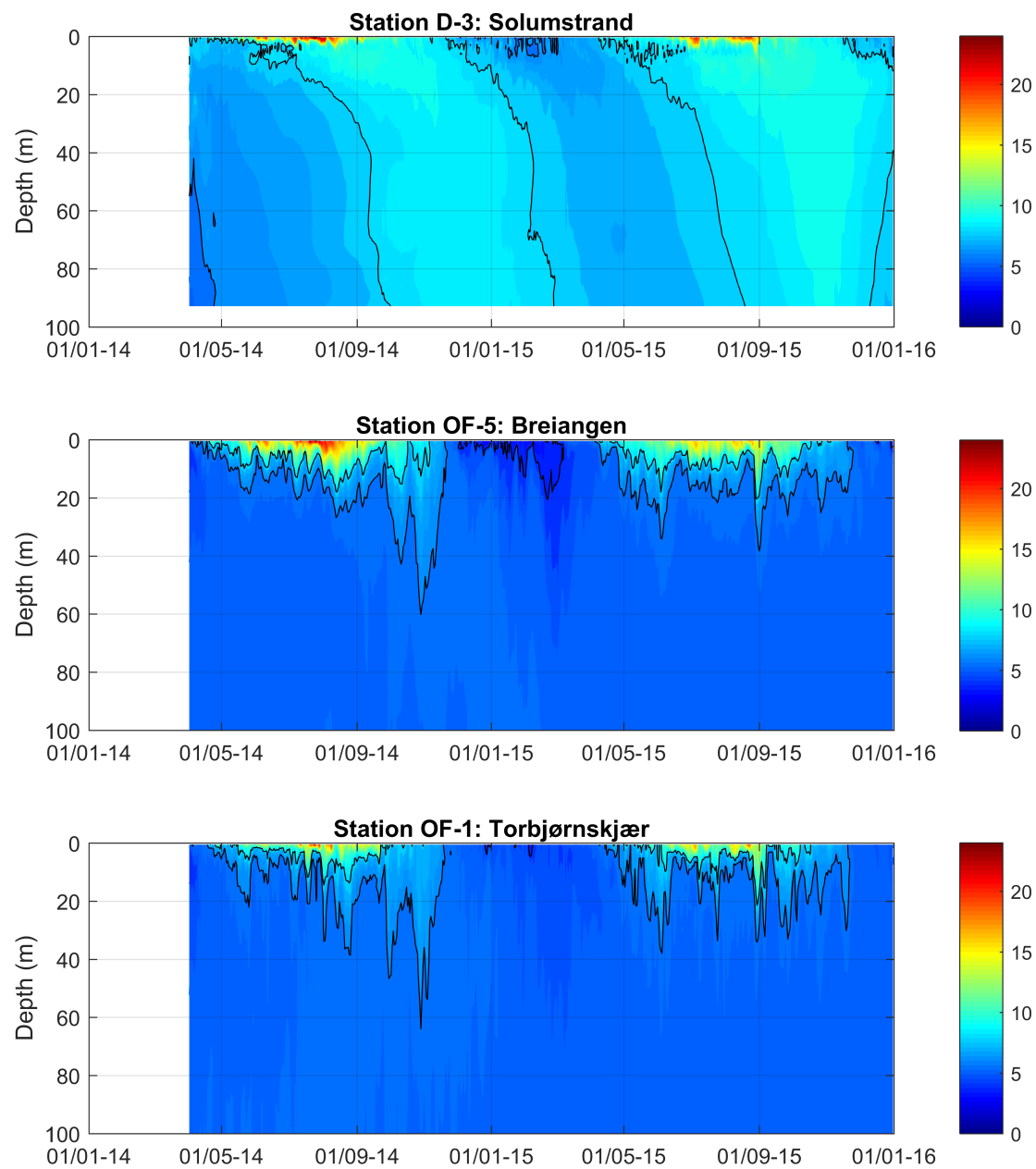


Figure 27: Modelled temperature at three stations in the Oslofjord. Contour lines mark 5 and 10 °C.

#### 4.3.2 Water temperature near Åsgårdstrand

The temperature observations from Scanmar AS are compared with simulated data extracted from 1.15 meters depth at approximately the same location as the observations.

Time series reveal that the simulated and observed temperature are in fairly good agreement (Fig. 28). During winter and spring, but the model underestimate the temperature in the summer and fall with a few degrees and 29). The model captures the timing of the daily variations in temperature, but seems to overestimate heating and cooling causing too large daily variations (Fig. 30).

2014 had a warmer summer than 2015. This is evident in both the observations and the simulations (Tab. 5). The summer months of 2014 also had the largest variance in both the observed and the simulated temperature during 2014 and 2015. Generally, the simulated monthly temperature had a larger variance than the observed monthly temperature. The mean of the observed and simulated temperatures are  $10.0^{\circ}\text{C}$  and  $8.6^{\circ}\text{C}$  respectively, while the variances are  $27.2^{\circ}\text{C}$  and  $21.1^{\circ}\text{C}$  respectively.

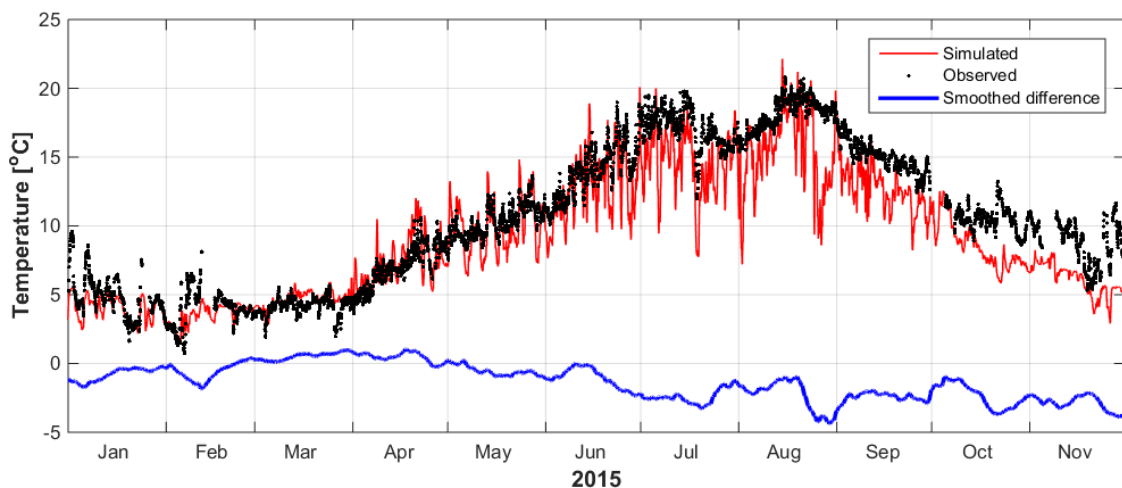


Figure 28: Time series of observed and simulated temperature at Åsgårdstrand. The difference is smoothed over 10 days.

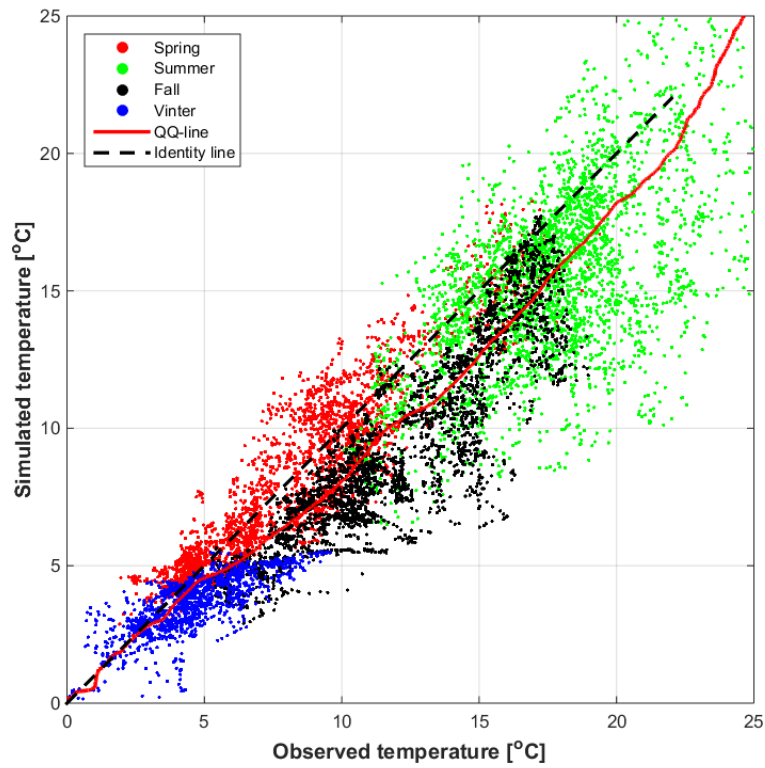


Figure 29: Combined QQ- and scatter plot of observed and simulated temperature at Åsgådstrand.

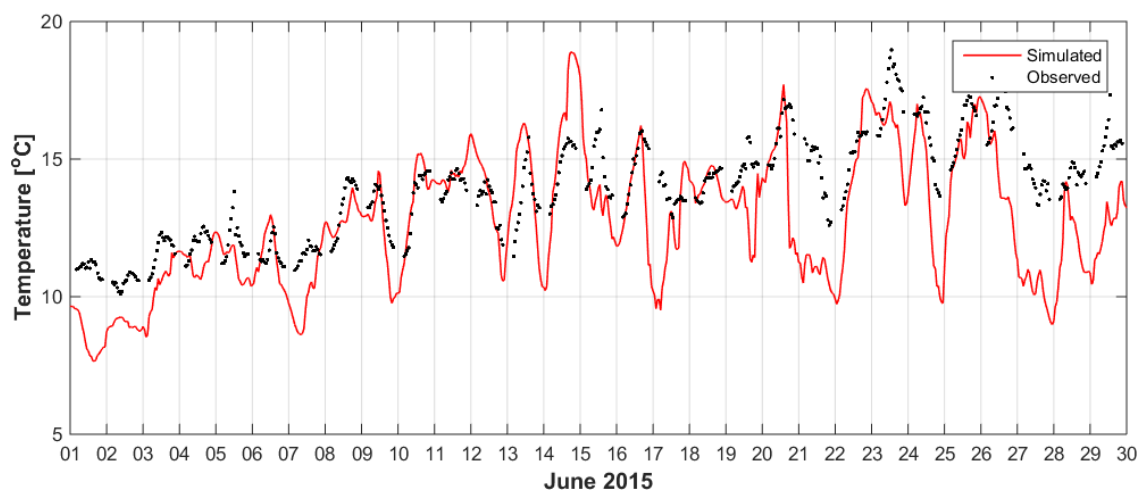


Figure 30: Time series of observed and simulated temperature at Åsgådstrand in June 2015.

Table 5: Monthly statistics for observed and simulated temperature at Åsgårdstrand.

		2014			2015		
		quantity	mean	variance	quantity	mean	variance
Jan	obs	558	2.5	6.2	558	4.9	2.5
	sim	745	-	-	745	4	0.7
Feb	obs	504	1.8	0.5	504	4	1.8
	sim	673	-	-	673	3.6	0.6
Mar	obs	496	3.7	0.6	496	4.2	0.4
	sim	745	-	-	745	4.7	0.3
Apr	obs	515	7.5	4.1	515	7	2.1
	sim	721	7.6	7.1	721	7.4	2.8
May	obs	544	12.1	9.3	544	10.3	1.3
	sim	745	11.3	10.4	745	9.9	3.5
Jun	obs	531	16.2	4.2	531	14	3.9
	sim	721	15.5	8.3	721	12.8	6
Jul	obs	558	20.2	10.5	558	17.1	2
	sim	745	17	24.3	745	14.6	5.1
Aug	obs	512	20	3.2	512	18.2	1.3
	sim	745	16.4	5.6	745	15.5	8.7
Sep	obs	536	16.3	1.9	536	15.1	1.2
	sim	721	12.9	8.9	721	12.7	2.5
Oct	obs	557	12.3	1.7	557	10.6	0.8
	sim	745	9	1.5	745	8.6	2.7
Nov	obs	540	8.3	2.9	540	8.8	2.4
	sim	721	6.3	2	721	6.1	1.3
Dec	obs	490	4.4	3.6	490	7.8	0.4
	sim	733	3.4	1.5	733	4.8	0.8

#### 4.3.3 Water temperature in the Inner Oslofjord

The observed and simulated temperature at three beaches in the Inner Oslofjord are in relatively good agreement (Fig. 31 - 32).

Close to the shoreline and only 40 cm under the surface, the temperature is heavily influenced by the weather situation and local circulation patterns.

The temperature differences during the day are larger in the model than in the observations. The observed temperature increases 1-3 degrees from 09:00 to 18:00 and is not measured during the night, while the modelled temperature increases up to six degrees from 06:00 to 23:00. The fact that temperature is not measured during the night, but only from 09:00 to 18:00, might explain differences in temperature rise during the day, but the difference might indicate too much heating in the model.

During the summer 2014 the model predicts higher temperatures at Sjøstrand than was observed. The observations in Hvalstrand have some of the same trends as the modelled temperature with temperatures up to 25 degrees. The air temperatures in 2014 was higher than in 2015 and resulted in higher water temperatures, especially in shallow areas.

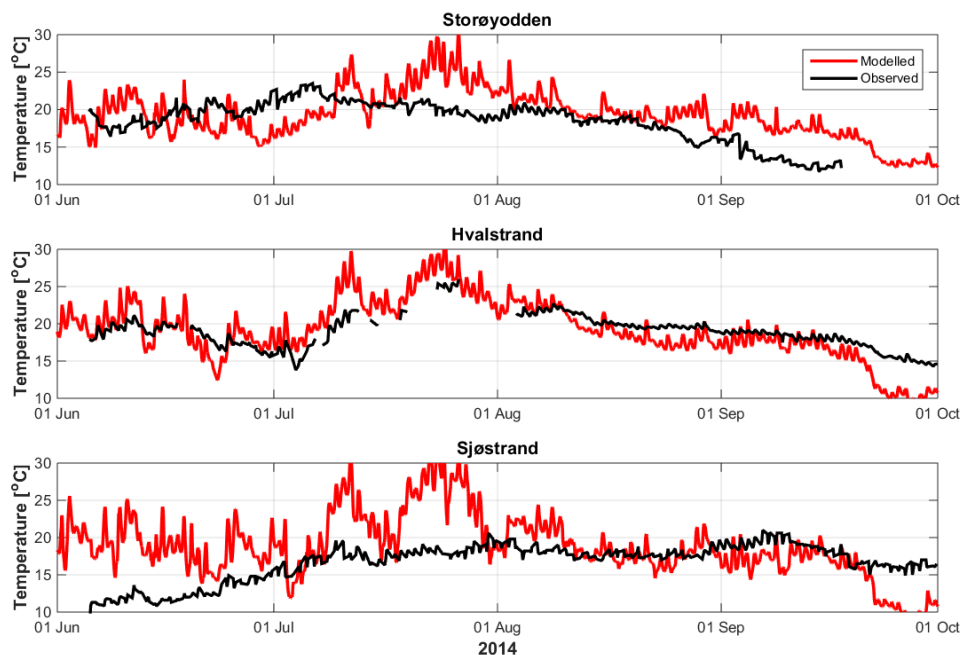


Figure 31: The observed and modelled temperature at three beaches in the Inner Oslofjord during the summer 2014

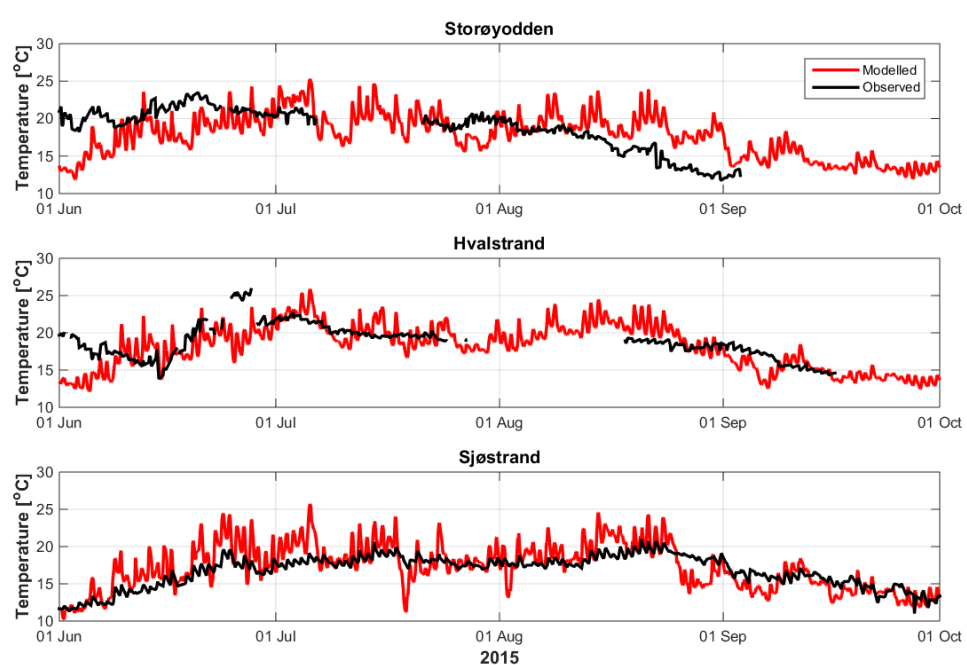


Figure 32: The observed and modelled temperature at three beaches in the Inner Oslofjord during the summer 2015

## 4.4 Drifting lanes

### 4.4.1 Godafoss

Since the time period of the model does not cover the time period when the container ship Godafoss ran aground, we have instead released drifters in our model from the position of the oil spill from Godafoss for a period of one year. We argue that over such a long period of time, there will be at least one weather and current situation similar to the weather and currents experienced during the Godafoss release. By showing the models ability to advect oil to the observed locations during a one year run, we at least show that our ocean model is capable of recreating the right drift patterns.

To simulate the drift of the oil, we have applied the open source trajectory-model OpenDrift. This is a trajectory model under development at MET Norway, and is described by its developers as "a software for modelling the trajectories and fate of objects or substances drifting in the ocean, or even in the atmosphere". It is distributed under a GPL v2.0 license, and is available on GitHub<sup>2</sup>.

The OpenDrift model was forced with currents from the FjordOs model and with wind from the Arome-MetCoOp 2.5km (Arome2.5) atmospheric model (the same atmospheric model was used as forcing when running the FjordOs hindcast). We have also provided daily mean currents from NorKyst-800m outside of the FjordOs-model, to properly treat the particles that are advected out of the FjordOs-model, so they can re-enter at the correct location. We can tune a number of parameters when running OpenDrift, e.g. random walk and the wind drift factor. Random walk was not used in our simulations of drifting lanes, and the wind drift factor was set to 0.01 (i.e. 1%). Modelled drifters has been released once per hour from April 1st 2015 to April 1st 2016, a total number of 8760 particles. The lifetime of each particle is set to 15 days, i.e. after 15 days the particle is deactivated. This is done to reduce the computational cost of advecting a large number of particles.

The results from the drift model can be viewed in Figure 33 - 35. In Figure 33, we show the number of hours from the particles were released until they reached different areas of the domain. Figure 34 show the likelihood of an area experiencing oil. This is done by counting the number of particles that has been inside each grid cell during the simulation, and presenting this as concentrations. Figure 35 depicts the same as the two previous figures, but only showing the values in the final position of each trajectory. This is to better visualise stranding sites. All these calculations are done on a 140m by 140m

---

<sup>2</sup><https://github.com/knutfrode/opendrift>

grid.

When comparing the results in Figure 33 - 35 to the observed oil in Figure 7, we clearly see that there are some similarities between the observations and the simulations. Especially by looking at Figure 35, right panel, we can see that a substantial number of particles are transported westward from the release position at Hvaler, and strand along the Vestfold coast, the islands around Tjøme, and the Færder lighthouse. We would also like to point out the very low number of particles that strand at the peninsula west of Stavern (the area far left in Figure 35). This corresponds well with where the oil was observed. In the left panel of Figure 35, we provide the shortest time from the release of particles, to stranding. We would like to point out two areas: Stavern (western part of Figure 35) and Bustein (northwest of the Færder lighthouse). In Figure 7, the oil at Bustein was discovered two days after the initial spill, while at Stavern (Korntin) the oil was observed after five days. This corresponds well with the timing in Figure 35.

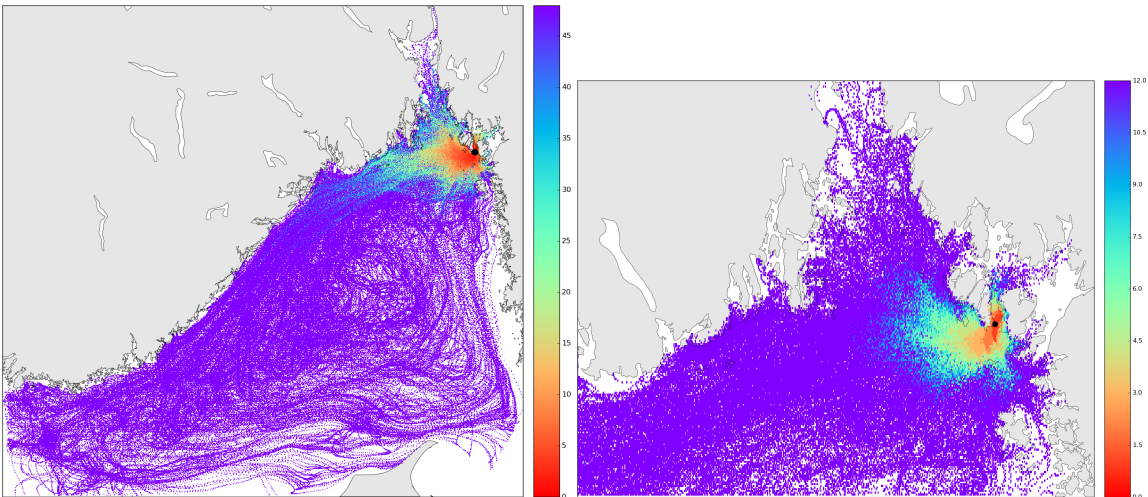


Figure 33: Number of hours from particle release, to particle is inside a given  $140 \times 140\text{m}$  area for the Godafoss scenario. Based on one year (April 1st 2015 - April 1st 2016) of simulations, with a maximum lifetime of 15 days of the released particles. This amounts to a total number of 8760 released particles. Please note the different scales of each figure.

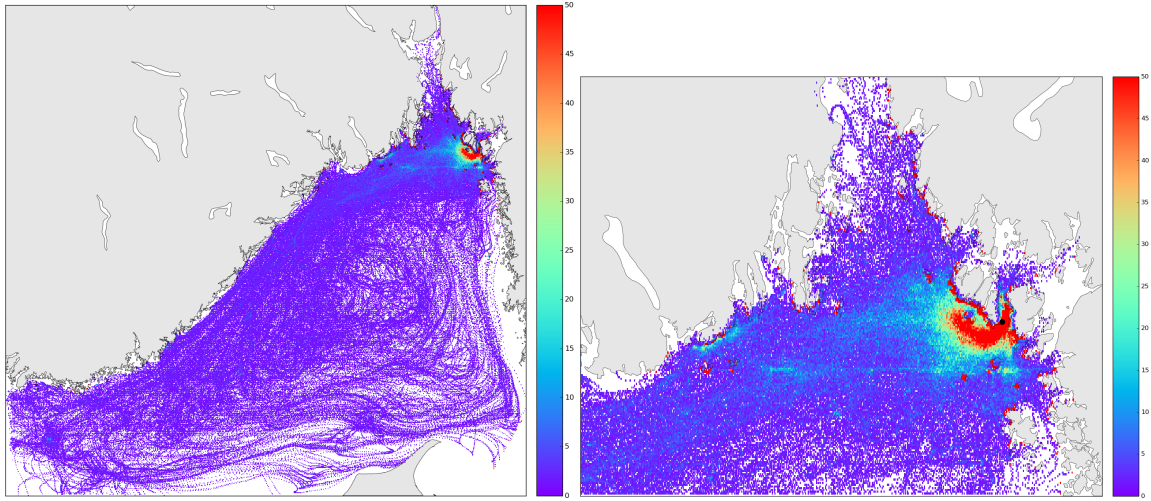


Figure 34: Same as Figure 33, but for number of particles that has been inside a given  $140 \times 140\text{m}$  area for the Godafoss scenario. Please note the different scales of each figure.

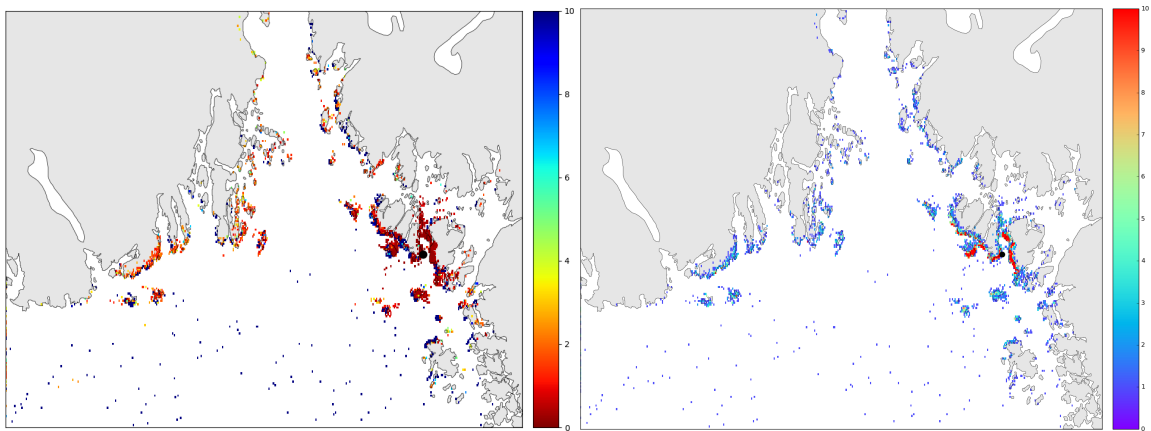


Figure 35: Similar to Figure 33 and 34, but only showing end position of each trajectory: Number of days from particle release (note different time scale) to particle in given area (left panels), and the number of particles that have been inside a given  $140 \times 140\text{m}$  area (right panel). Please note the different scales of each figure.

#### 4.4.2 Surface drifters

We evaluate the models ability to recreate the drifter trajectories by using a skill-score, as described in *Liu and Weisberg* (2011):

$$s = \sum_{i=1}^N d_i / \sum_{i=1}^N l_{oi}$$

$$ss = \begin{cases} 1 - \frac{s}{n} & (s \leq n) \\ 1 & (s > n) \end{cases}$$

where  $n$  is a tolerance threshold,  $d_i$  is the separation distance between the modelled and observed endpoints of the Lagrangian trajectories at time step  $i$  after the initialisation (virtual particle release),  $l_{oi}$  is length of the observed trajectory, and  $N$  is the total number of time steps.

A skill-score of 1 means a perfect match, while a score of 0 means no skill. The skill-score for each drifter compared to trajectories from OpenDrift based on both the FjordOs and NorKyst-800m models is given in Table 6, 7, 8, and 9. For simulated trajectories during the September 2015 cruise (Table 6 and 7), both currents and wind drift has been applied, while for the trajectories of September 2014 (Table 8 and 9) only currents have been applied to produce the trajectories.

Examination of the values for skill-score, and visual inspection of the trajectories themselves, do not provide a clear conclusion on which ocean model performs better. During the September 2014 release, the FjordOs model performs better than the NorKyst-800m, but there is a clear weakness here since we do not have hourly data from NorKyst-800m available. Also, there are only two drifters. The FjordOs model has the highest skill-score based on both hourly and daily average data, and was the only model to transport the drifters as far south as the observed drift. Based on this, we think it is safe to conclude that the FjordOs model had an overall current situation that was close to the real situation. The currents in NorKyst-800m is believed to be too weak during this drifter release.

During the September 2015 cruise we released 10 drifters. The NorKyst-800m model has an overall higher skill-score than FjordOs when we take into account the entire trajectory, and also when we only consider the first hour of the trajectory. When we do the visual comparison between the trajectories in Figure 36 - 38, it is very tempting to point out that the trajectories based on the FjordOs model more often compares well to the observed trajectory than what the one based on NorKyst-800m does, but we will leave this

<b>Drop no.</b>	<b>FjordOs</b>	<b>NorKyst-800m</b>
1	0.77 (11)	0.68 (11)
4	0.78 (2)	0.53 (1)
6	0.00 (3)	0.84 (11)
8	0.82 (21)	0.58 (21)
51	0.58 (3)	0.73 (15)
52	0.38 (4)	0.50 (1)
61	0.58 (3)	0.70 (8)
91	0.51 (8)	0.50 (12)
101	0.61 (15)	0.78 (15)
102	0.59 (6)	0.75 (7)
<b>Avg.</b>	<b>0.56</b>	<b>0.66</b>

Table 6: Skill-score of drifter trajectories released during the September 2015 cruise. We have used a tolerance threshold  $n = 2$  to get positive values for most trajectories. The number in parenthesis indicates how many hours the model trajectory is.

up to the reader to decide.

<b>Drop no.</b>	<b>FjordOs</b>	<b>NorKyst-800m</b>
1	0.17	0.14
4	0.55	0.45
6	0.07	0.46
8	0.00	0.00
51	0.49	0.58
52	0.37	0.47
61	0.49	0.58
91	0.73	0.67
101	0.63	0.78
102	0.87	0.77
<b>Avg.</b>	<b>0.43</b>	<b>0.49</b>

Table 7: Same as Table 6, but only considering the first hour of the trajectory.

<b>Drop no.</b>	<b>FjordOs 1h</b>	<b>NorKyst-800m 24h</b>
1	0.79 (15)	0.73 (15)
2	0.84 (19)	0.76 (19)
<b>Avg.</b>	<b>0.81</b>	<b>0.75</b>

Table 8: Same as Table 6, but for the drifter release during the September 2014 cruise. Please note that the FjordOs model has hourly resolution for current data, while the NorKyst-800m model has daily averages only. This is due to the availability of the data from NorKyst-800m.

<b>Drop no.</b>	<b>FjordOs 24h</b>	<b>NorKyst-800m 24h</b>
1	0.85 (15)	0.73 (15)
2	0.91 (19)	0.76 (19)
<b>Avg.</b>	<b>0.88</b>	<b>0.75</b>

Table 9: Same as Table 8, but modelled trajectories from FjordOs are based on daily average ocean currents to get a more fair comparison between the models.

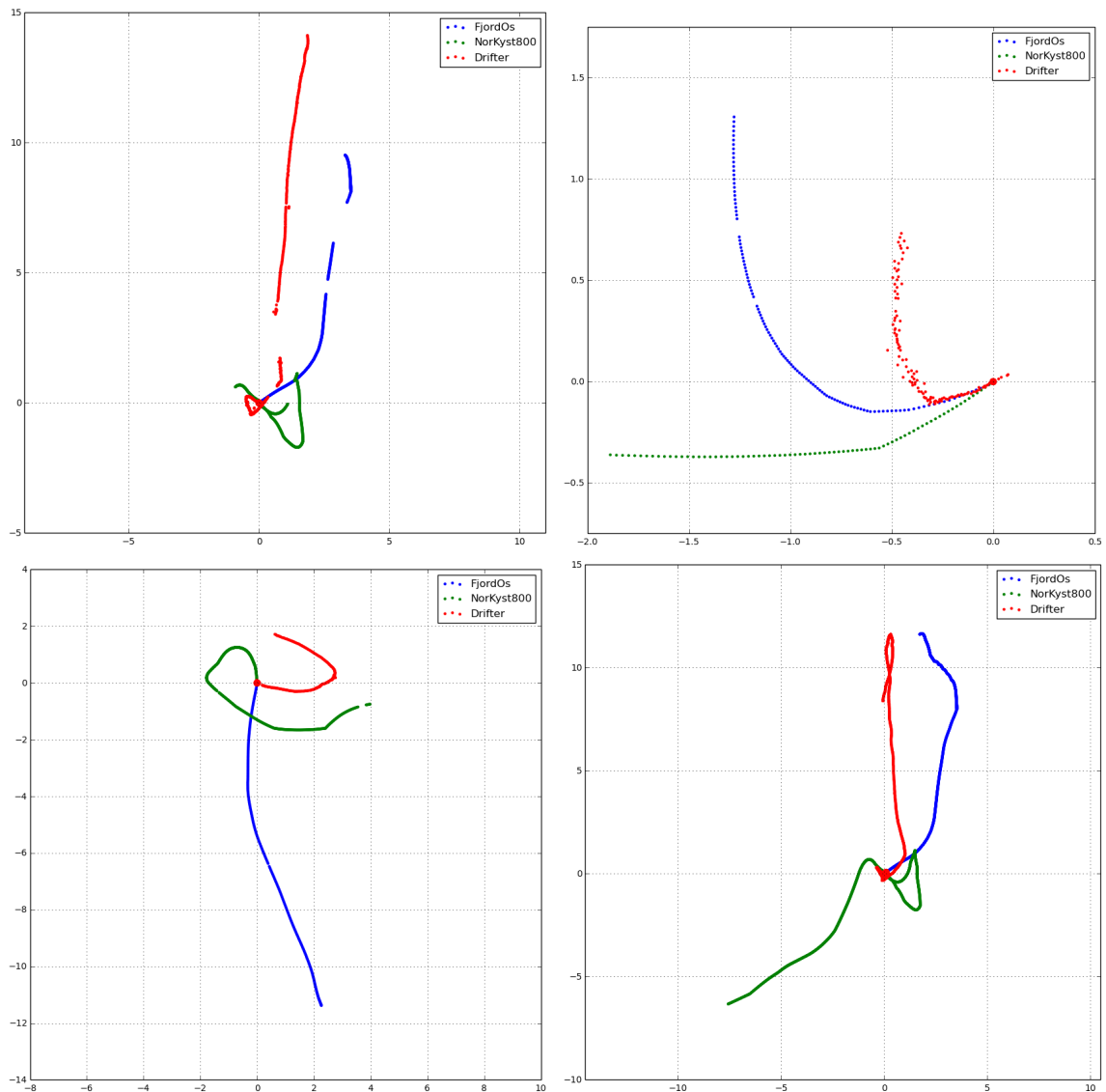


Figure 36: Figures showing comparisons of modelled and observed drifter trajectories during the September 2015 cruise. Modelled trajectories has been simulated using both NorKyst-800m and the FjordOs model. Values along X- and Y-axis indicate distance in kilometres. Top-left is drop 1, top-right is drop 4, bottom-left is drop 6 and bottom-right is drop 8.

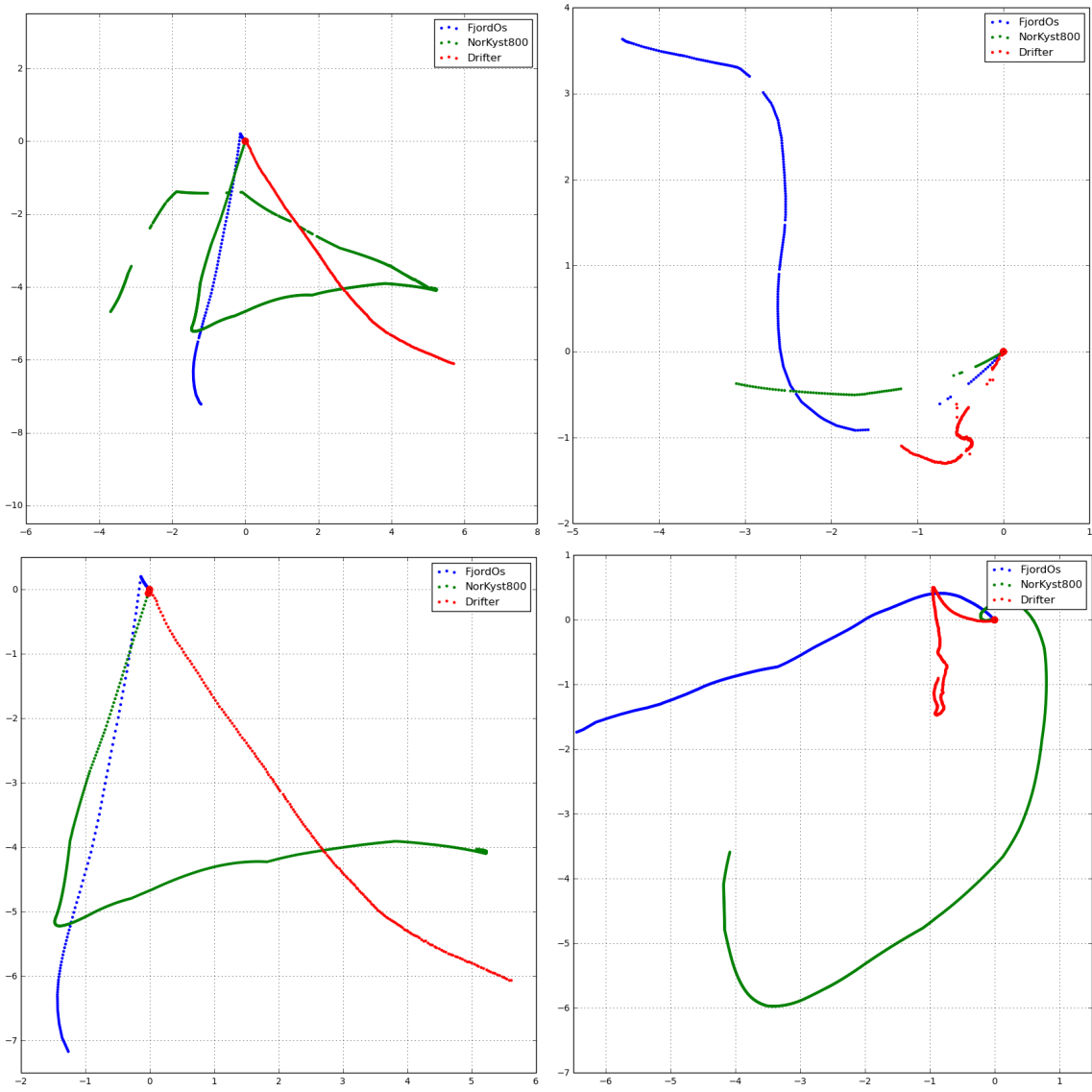


Figure 37: Same as Figure 36, but for the following drifters: Top-left is drop 51, top-right is drop 52, bottom-left is drop 61 and bottom-right is drop 91.

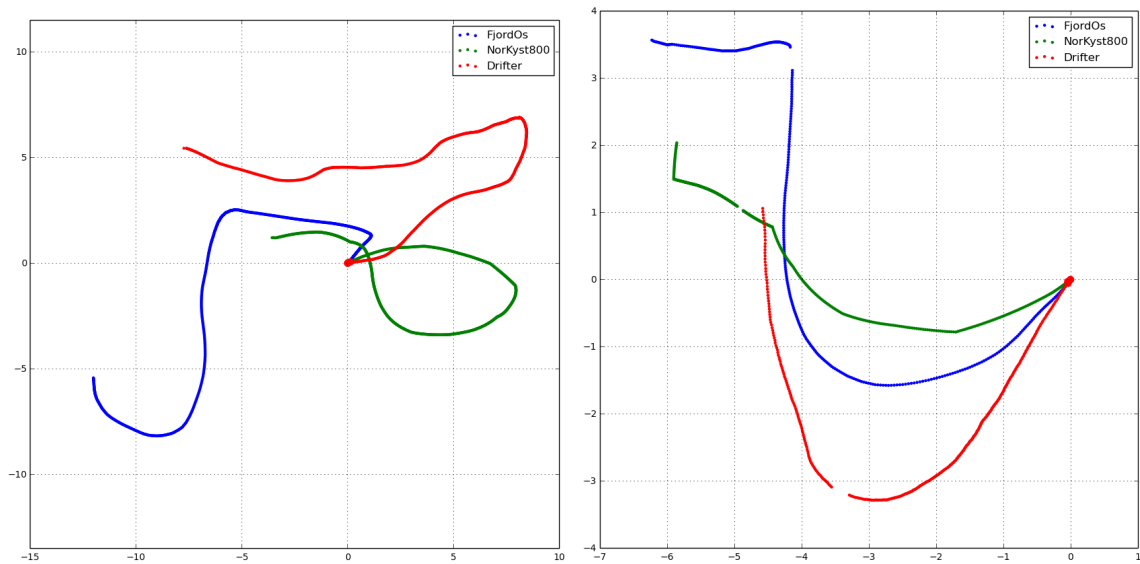


Figure 38: Same as Figure 36 and 37, but for the following drifters: Left is drop 101 and right is drop 102.

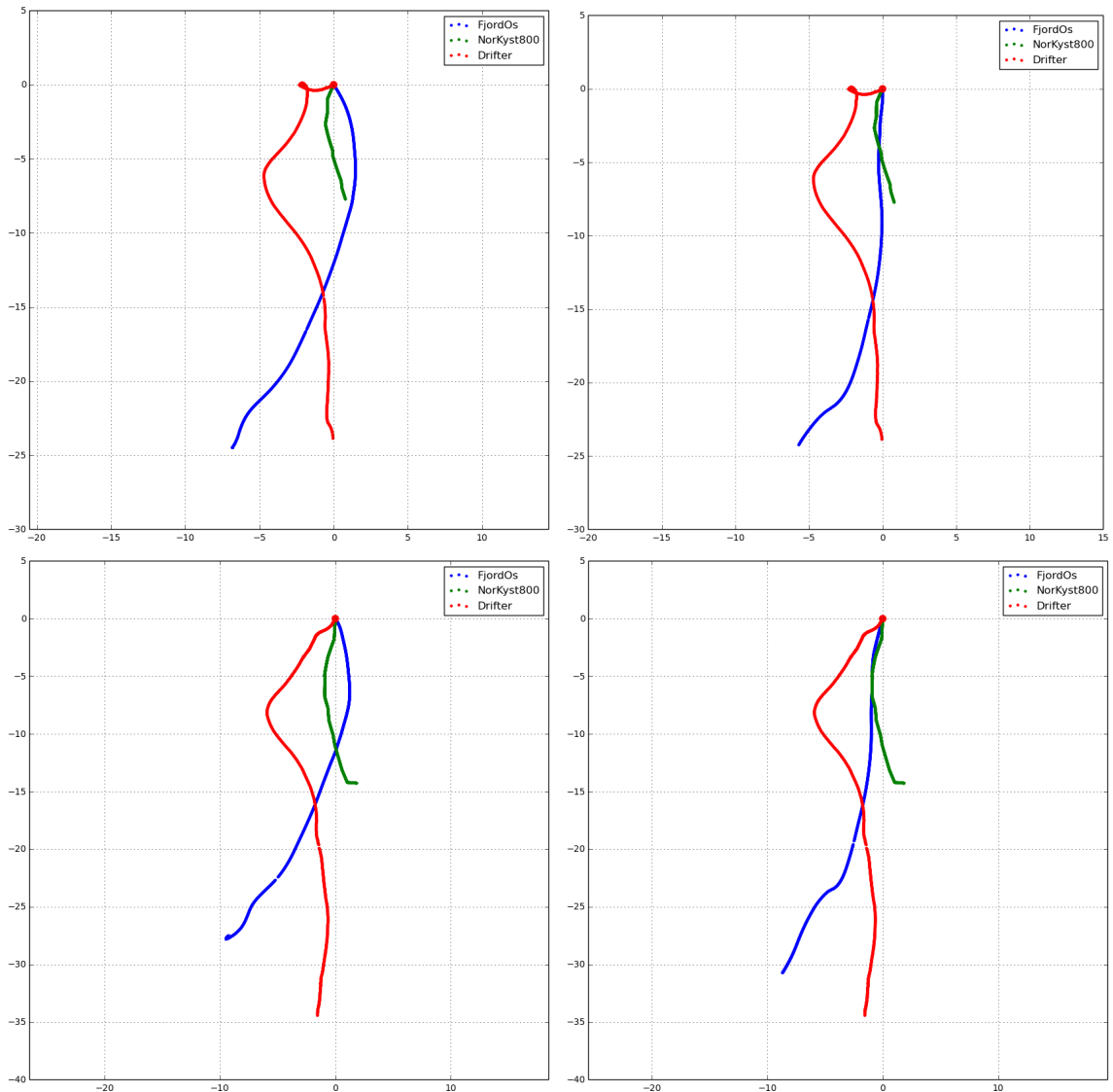


Figure 39: Same as Figure 36, but showing the September 2014 release. Top-left is drop 1, top-right is drop 1 based on 24h average data for FjordOs, bottom-left is drop 2 and bottom-right is drop 2 based on 24h average data for FjordOs.

## **5 Summary and final remarks**

## Acknowledgements

The present research and development is mostly funded by the the regional research funds Oslofjordfondet (Research grant no. 226022). We gratefully acknowledge the support. Smaller contributions from MET Norway, NIVA, HSN, Kystverket and Exxon are also appreciated.

## Appendix

### Driftling lanes from the Slagen refinery

A part of the FjordOs project has been to examine how known, and potential, oil spills would spread out in the Oslofjord. The Slagen refinery at Slagentangen is owned by ExxonMobil, and is described as following on their webpage<sup>3</sup>: "Slagen Refinery is situated on the west bank of the Oslofjord about 5 nautical miles south of Horten. The marine terminal consists of a pier about 500 m long with loading/discharging berths on both sides. To the south of the long pier there is a small harbour where mooring boats and oil recovery equipment are kept. The terminal and its near surroundings are owned and controlled by Esso Norge AS. It has its own Harbour Office with Marine Supervisors on duty 24 hours a day." and "The Slagen Marine Terminal has approximately 800 tanker calls a year with size variation 100 to 250 000 DWT. The annual import of Crude oil (mainly from the North sea) and Blendstock is about 6.5 mill.  $m^3$  and about 5.7 mill.  $m^3$  petroleum products are shipped out."

To model the spread of oil from a potential spill at Slagentangen we have used the same approach as in Section 4.4.1. It is very important to point out that the work done in this appendix is not sufficient to be used for any contingency planning or other work on possible oil spill scenarios. It should be viewed as a "teaser" on possible future work that could be used for contingency planning of unwanted releases of substances from anywhere within the Oslofjord.

Figure 40 shows the release position of the particles used in the simulation marked with a black dot. The left panel show the shortest number of hours from the time of the particle release to a particle is in a given position. The right panel show the corresponding concentrations. When viewing the zoomed in figures (lower figures), it is evident that the coastline of the ocean model does not perfectly match the real coastline, and also the OpenDrift model will at times advect particles onto land. This is linked to the length of the time step used in OpenDrift. A more thorough work on potential oil spills should address these issues. When looking at the area closest to the release position, it clearly shows that most particles are transported towards the southeast, and this is also the direction of which

---

<sup>3</sup>[http://www.exxonmobil.no/en-NO/company/operations/operating-locations/slagen-refinery?sc\\_lang=en-NO](http://www.exxonmobil.no/en-NO/company/operations/operating-locations/slagen-refinery?sc_lang=en-NO), (visited 26.01.2017)

the particles are transported fastest. This compares well to the observations of currents outside Slagen in Figure 18. Figure 41 show the end positions of each trajectory, and the corresponding shortest time from release to that position, and concentration.

This sort of maps could be made and categorised by weather pattern or another known factor, and in turn e.g. be used in the unlikely event of a spill in the time between the spill happening, and the forecast of oil drift is received.

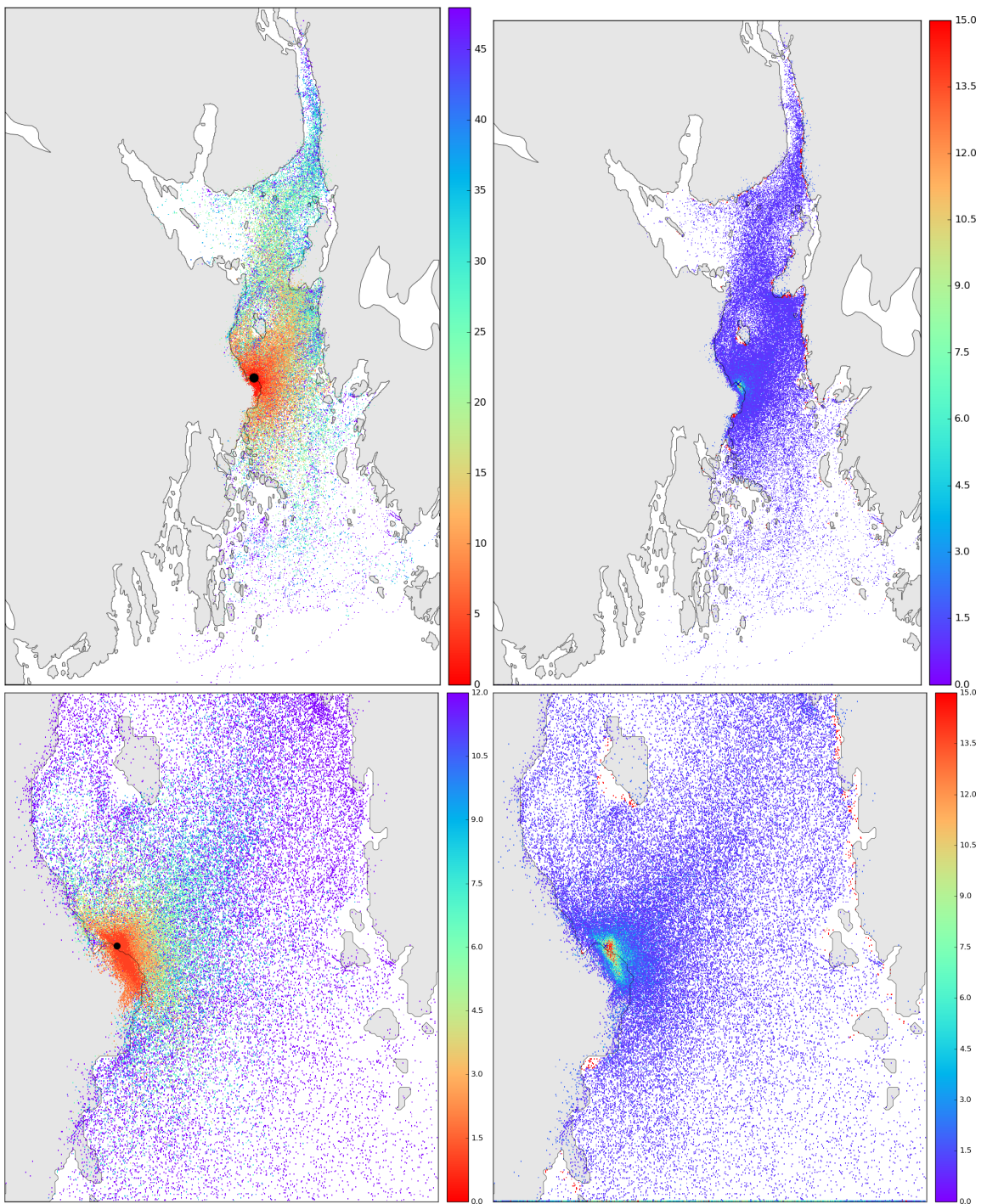


Figure 40: Slagentangen. Number of hours from particle release, to particle in given area (left panels), and the number of particles that has been inside a given 140x140m area (right panels). Based on one year (April 1st 2015 - April 1st 2016) of simulations, with a maximum lifetime of 15 days of the released particles. This amounts to a total number of 8760 released particles. Please note the different scales of each figure.

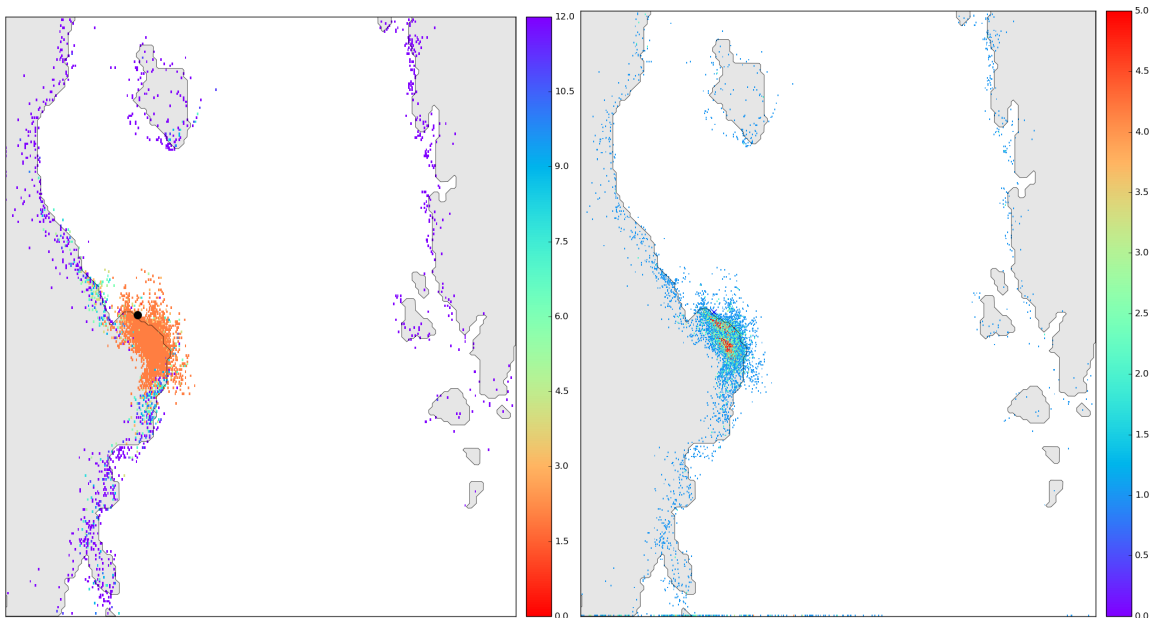


Figure 41: Slagentangen. For end position of each trajectory: Number of hours from particle release, to particle in given area (left panel), and the number of particles that has been inside a given 140x140m area (right panel). Based on one year (April 1st 2015 - April 1st 2016) of simulations, with a maximum lifetime of 15 days of the released particles. This amounts to a total number of 8760 released particles. Please note the different scales of each figure.

## References

- Baalsrud, K., and J. Magnusson (2002), *Indre Oslofjord (in Norwegian)*, Fagrådet for Indre Oslofjord.
- Haidvogel, D. B., H. Arango, P. W. Budgell, B. D. Cornuelle, E. Curchitser, E. D. Lorenzo, K. Fennel, W. R. Geyer, A. J. Hermann, L. Lanerolle, J. Levin, J. C. McWilliams, A. J. Miller, A. M. Moore, T. M. Powell, A. F. Shchepetkin, C. R. Sherwood, R. P. Signell, J. C. Warner, and J. Wilkin (2008), Ocean forecasting in terrain-following coordinates: Formulation and skill assessment of the Regional Ocean Modeling System, *J. Comput. Phys.*, 227(7), 3595–3624, doi:<http://dx.doi.org/10.1016/j.jcp.2007.06.016>.
- Hjelmervik, K., N. M. Kristensen, A. Staalstrøm, and L. P. Røed (2017), A simple approach to adjust tidal forcing in fjord models, *Intended for Ocean Dynamics, (submitted)*.
- Hjelmervik, K. B., N. M. Kristensen, and A. Staalstrøm (2016), Comparison of simulations and observations in the oslofjord. fjordos technical report no. 3, *MET Report 13*, Norwegian Meteorological Institute, MET Norway, P.O.Box 43 Blindern, NO-0313 Oslo, Norway.
- Liu, Y., and R. H. Weisberg (2011), Evaluation of trajectory modeling in different dynamic regions using normalized cumulative lagrangian separation, *Journal of Geophysical Research: Oceans*, 116(C9).
- Pawlowicz, R., B. Beardsley, and S. Lentz (2002), Classical tidal harmonic analysis including error estimates in MATLAB using T\_TIDE, *Computers and Geosciences*, 28(8), 929–937.
- Røed, L. P., N. M. Kristensen, K. B. Hjelmervik, and A. Staalstrøm (2016), A high-resolution, curvilinear roms model for the oslofjord. fjordos technical report no. 2, *MET Report 4*, Norwegian Meteorological Institute, MET Norway, P.O.Box 43 Blindern, NO-0313 Oslo, Norway.
- Shchepetkin, A. F., and J. C. McWilliams (2003), A method for computing horizontal pressure-gradient force in an oceanic model with a nonaligned vertical coordinate, *J. Geophys. Res.*, 108, 3090, doi:10.1029/2001JC001047.

Shchepetkin, A. F., and J. C. McWilliams (2005), The Regional Ocean Modeling System (ROMS): A split-explicit, free-surface, topography-following coordinate ocean model, *Ocean Modelling*, 9, 347–404.

Shchepetkin, A. F., and J. C. McWilliams (2009), Correction and commentary for "Ocean forecasting in terrain-following coordinates: Formulation and skill assessment of the regional ocean modeling system" by Haidvogel et al., *J. Comp. Phys.* 227, pp. 3595–3624, *J. Comp. Phys.*, 228(24), 8985 – 9000, doi:10.1016/j.jcp.2009.09.002.

Staalstrøm, A., and P. Ghaffari (2015), Current conditions in the oslofjord - focus on current strength along the bottom, *Technical Report SNO 6799-2015*, Norwegian Institute for Water Research, NIVA, Gaustadalléen 21, NO-0349 Oslo, Norway.

Staalstrøm, A., and K. Hjelmervik (2017), Strømforholdene i innløpet til drammensfjorden (in norwegian), *Vann (in review)*, -, -.